Characterizing human Nogo-66 receptor 1 interactions with reovirus by cryo-EM and receptor mutagenesis

by

Olivia L. Welsh

B.S. Immunology and Infectious Disease, The Pennsylvania State University, 2019

Submitted to the Graduate Faculty of the

School of Public Health in partial fulfillment

of the requirements for the degree of

Master of Science

University of Pittsburgh

2023

UNIVERSITY OF PITTSBURGH

SCHOOL OF PUBLIC HEALTH

This thesis was presented

by

Olivia L. Welsh

It was defended on

May 5, 2023

and approved by

Robbie B. Mailliard, PhD, Visiting Associate Professor, Department of Medicine,
University of Pittsburgh, School of Medicine

Amy Hartman, PhD, Associate Professor, Department of Infectious Diseases and Microbiology,
University of Pittsburgh, School of Public Health

Terence S. Dermody, MD, Professor, Department of Pediatrics,
University of Pittsburgh, School of Medicine

Characterizing human Nogo-66 receptor 1 interactions with reovirus by cryo-EM and receptor mutagenesis

Olivia L. Welsh, MS

University of Pittsburgh, 2023

Human Nogo-66 receptor 1 (NgR1) modulates axonal plasticity in the brain and serves as a receptor for mammalian orthoreovirus (reovirus). To elucidate the mechanism by which this receptor engages reovirus, we conducted cryo-electron microscopy (cryo-EM) analyses of soluble NgR1 bound to reovirus. A three-dimensional (3D) cryo-EM reconstruction reveals that NgR1 engages two protomers of the σ3 viral capsid protein. However, the resolution of the map is insufficient to confirm critical contact residues. We placed known reovirus and NgR1 crystal structures into the 3D reconstruction and used this reovirus-NgR1 model to guide mutagenesis. We engineered a panel of σ3 mutants within the proposed NgR1-binding region and assessed σ3 binding to NgR1, however no σ3 residue substitution was sufficient to disrupt NgR1 binding. We also engineered NgR1 mutants in which NgR1 residues in high-proximity or low-proximity to reovirus σ3 were exchanged with arginine or glutamate. Mutation of most high-proximity residues disrupted reovirus binding and infection of NgR1-expressing cells. However, mutation of low-proximity residues infrequently diminished binding and infectivity. Placement of residues required for reovirus binding onto the NgR1 structure revealed a binding footprint on both the concave and convex surfaces of NgR1. Although human NgR1 shares sequence similarities with family member NgR2 and homolog murine NgR1, only human NgR1 is a functional reovirus receptor. We therefore sought to identify key residues at the reovirus-binding interface of human NgR1 that also may serve as polymorphic sites that impede reovirus binding to NgR2 or murine NgR1. We

engineered a panel of NgR1-to-NgR2 mutants and also murine-to-human NgR1 mutants within the convex, non-conserved interface proximal to reovirus σ3. Mutation of these residues was not sufficient to diminish reovirus binding in loss-of-function studies, or confer receptor functionality in gain-of-function studies. Collectively, these findings validate the 3D cryo-EM reconstruction and provide insight into the mechanism used by reovirus to engage NgR1.

Table of Contents

List of Tables

List of Figures

1.0 Introduction

1.1 Viral encephalitis as a public health concern

Encephalitis in children is a worldwide public health concern. This illness is characterized by infection of the brain and often results in lifelong neurologic dysfunction (6). While encephalitis can be caused by multiple pathogens, most cases are due to viral infections (7). As virus-induced inflammation of the central nervous system (CNS) can lead to irreparable brain injury and even death, viral encephalitis is an important target for therapeutic drug development. To best inform therapeutic approaches to mitigate viral encephalitis, it is imperative to understand how viruses infect the CNS. Mammalian orthoreovirus (reovirus) causes strain- and age-dependent encephalitis and serves as a robust experimental system to study neuropathic viruses in mice. Although reovirus rarely causes severe disease in humans, it is used as a model pathogen to study how viruses infect the developing CNS. In this study, we discovered a new binding mechanism used by reovirus to engage a neuronal receptor. This newly described attachment interaction furthers our understanding of viral entry into neurons and may inform development of therapeutic interventions to prevent and treat viral encephalitis and virus-induced neuronal injury.

1.2 Reovirus introduction and biology

The first step in the life cycle of every virus is to attach to host cell receptors. Without this step, the virus is incapable of accessing the intracellular environment required for viral replication.

To enter host cells, viruses use capsid proteins to interact with host attachment factors and entry receptors. Viral capsid proteins often extend from the virus surface to facilitate interactions with host cells. Following host cell binding, virus can enter cells using a variety of mechanisms to initiate a replication cycle.

Reovirus infects a wide variety of mammals and causes disease in the very young (8). Although reovirus readily infects humans, disease is rare and often asymptomatic (8, 9). However, reovirus infection causes severe neurologic disease in newborn rodents, which serve as excellent models to study viral neuropathogenesis. In mice, serotype 1 (T1L) reovirus establishes infection in the lung or intestine and disseminates via the bloodstream to infect ependymal cells in the brain, causing a non-lethal hydrocephalus. Serotype 3 (T3D) reovirus uses both hematogenous and neural routes of dissemination following primary infection and spreads to the brain to infect neurons and cause lethal encephalitis (10). Although routes of dissemination used by reovirus have been described, the mechanism by which reovirus infects CNS cells is not well understood.

Reovirus forms nonenveloped virions composed of two concentric shells, the outer capsid and inner core. The outer capsid facilitates viral attachment and entry into host cells, and the core protects the viral genome and contains the enzymatic activities required for viral genome transcription and replication (8). Several host molecules have been identified as reovirus receptors. Sialic acids are attachment factors bound by reovirus outer-capsid protein σ1 (11), which extends from the virion surface and dictates serotype-dependent patterns of dissemination, tropism, and disease (12). Reovirus attachment protein σ1 also binds junctional adhesion molecule-A (JAM-A), which allows hematogenous spread within the host. However, binding to sialic acid or JAM-A is not required for reovirus replication in the intestine or brain (13), suggesting that reovirus uses other host receptors to infect these sites. Nogo-66 receptor 1 (NgR1) was identified as a reovirus

receptor in a whole-genome siRNA screen and found to confer binding to and infection of non-susceptible cells following plasmid transfection (14). Studies of this neuronally expressed receptor may enhance our understanding of reovirus replication in the CNS and its capacity to cause encephalitis.

1.3 NgR1 introduction and biology

NgR1 is expressed on the surface of neurons and promotes reovirus infection of cultured neurons prepared from fetal mice (14, 15). Instead of engagement by the well-characterized reovirus attachment protein, σ1, NgR1 instead binds to outer-capsid protein σ3 (16). Reovirus σ3 is a virion structural protein that, with proteins μ1 and λ2, forms the bulk of the reovirus outer capsid (**Figure 1A**) (1, 2). NgR1 engagement of σ3 is particularly interesting, as σ3 has not been implicated as a viral ligand for host receptors. Since NgR1 contributes to neuronal function, understanding how reovirus engages this receptor may have broader therapeutic implications.

NgR1 is a member of the Nogo receptor family, which also includes NgR2 and NgR3 (3). NgR1 is the best-characterized family member, and it functions in CNS neurons to mediate axon growth, synaptic plasticity, and neuronal regeneration (17, 18). These functions of NgR1 are mediated by binding to three distinct myelin-associated inhibitor (MAI) ligands; Nogo-66, myelin-associated glycoprotein (MAG), and oligodendrocyte myelin glycoprotein (OMgP) (3) (**Figure 1B**). Although structurally dissimilar, these three natural ligands of NgR1 are thought to bind a conserved region of the receptor. A large leucine-rich repeat (LRR) region of NgR1 forms a crescent-shaped domain in the center of the protein. Several NgR1 residues required for binding to Nogo-66, MAG, and OMgP were identified using alanine-scanning mutagenesis (3) and are

shown mapped onto the NgR1 LRR domain structure in Figure 1C. These critical residues are largely localized to the concave face of the LRR domain of NgR1. We hypothesize that reovirus outer-capsid protein σ3 also engages NgR1 using this functionally and structurally conserved region.

1.4 Cryo-EM structure of reovirus and NgR1

In a collaborative study with the laboratories of Drs. B. V. V. Prasad and Thilo Stehle, we determined the structure of reovirus in complex with NgR1, which revealed an unusual method of reovirus-receptor engagement. Reovirus virions were incubated with a soluble form of NgR1 containing the LRR domain, which we found was sufficient to bind reovirus (16). The virus-receptor complexes were embedded in vitreous ice and imaged using cryo-electron microscopy (cryo-EM). Several hundred particles were averaged to visualize the interaction between NgR1 and σ3 at 8.9 Å resolution. Unlike the common, well-described binding mechanism in which viruses use an extended capsid protein to interact with a host receptor, we observed that reovirus uses a non-extended capsid protein to interact with two sides of a host receptor (**Figure 1D**). Our reconstruction suggests that reovirus employs a receptor-engagement method similar to the canyon hypothesis formulated for rhinovirus-receptor interactions, in which host receptors engage a concavity on the viral surface rather than an extended viral attachment protein (19). This binding mechanism has been described for a variety of viruses including adenovirus (20), picornaviruses (21), and rotavirus (22), among others.

Although the structure of NgR1 bound to reovirus virions was encouraging, the relatively low resolution of the cryo-EM reconstruction does not reveal side chains to identify with certainty

the specific NgR1 residues used to engage reovirus. Therefore, it was necessary to validate these results using alternative strategies to confirm that residues predicted to be engaged on each NgR1 surface are required for reovirus binding.

In this study, we validated residues on the NgR1 surface required for binding and infection by reovirus. First, a model was constructed by superimposing known protein structures of NgR1 and σ3 into the cryo-EM density map of NgR1 in complex with reovirus. We identified residues in σ3 proximal to NgR1 and evaluated whether alteration of a selected number of these residues would diminish NgR1 binding using protein-protein interaction experiments. Additionally, we identified NgR1 residues proximal to neighboring σ3 molecules and determined whether these residues are required for reovirus binding and infection using a scanning mutagenesis approach. We also assessed whether exchange of NgR1 and NgR2 residues at polymorphic sites as well as exchange of human and murine NgR1 residues at polymorphic sites would alter reovirus binding and infection. By confirming the importance of individual residues in NgR1 for reovirus binding and infection, we were able to validate the cryo-EM structural model and describe in detail the engagement of NgR1 and its newly identified viral ligand, reovirus σ3.

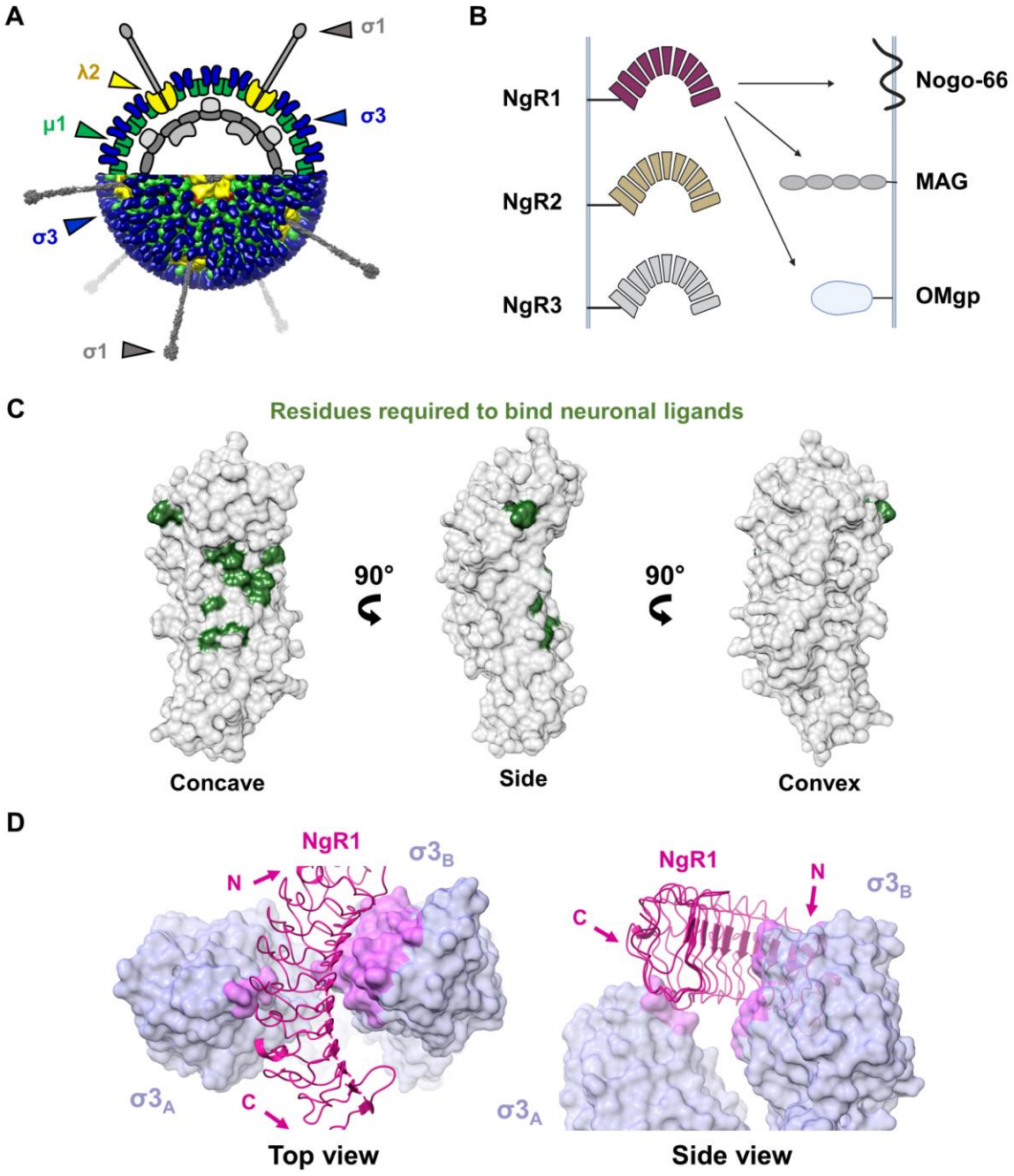

Figure 1. Reovirus binds the neuronal receptor, NgR1.

(**A**) Schematic of the reovirus virion showing viral outer-capsid proteins. Reovirus σ1 (gray), σ3 (blue), μ1 (green), and λ2 (yellow) proteins are depicted in cartoon (top) and surface-shaded protein (bottom) formats (1, 2). Interior structural proteins are depicted in gray. (**B**) Schematic showing NgR1 expression on neurons and engagement of myelin-associated ligands, including Nogo-66, MAG, and OMgp. NgR1 family members, NgR2 and NgR3, are included for comparison. (**C**) Residues required for binding (green) to Nogo-66, MAG, and OMgp (3) are mapped onto a surface-rendering of NgR1 (gray) amino acids 25-310 (of 447) (*1ozn*, (4)). (**D**) Crystal structure coordinates for NgR1 (*1ozn*) and reovirus outer-capsid protein σ3 (*1jmu*, (5)) were docked into the cryo-EM reconstruction and reveal that NgR1 (magenta ribbon tracing) engages two protomers of σ3 (blue surface-rendered), labeled $\sigma3_A$ and $\sigma3_B$. Surfaces of σ3 within 5 Å of NgR1 are shaded in magenta. Top (left) and side (right) views are shown; N'- and C'-termini of NgR1 are indicated.

2.0 Specific Aims

2.1 Specific aim I. Characterize reovirus residue interactions of σ3 and NgR1 within the proposed binding region

Rationale: The cryo-EM model of reovirus in complex with NgR1 reveals two σ3 protomers flanking NgR1. One flanking σ3 protein interacts closely with the concave, MAI-binding domain of NgR1. Due to its proximity to the well-characterized binding domain of NgR1, reovirus likely engages NgR1 within this region.

Hypothesis: Mutation of σ3 residues within the proposed binding region of NgR1 will diminish protein:protein interactions between σ3 and NgR1. To characterize targeted residue interactions, protein binding assays between NgR1 and wildtype or mutagenized σ3 will be completed.

2.2 Specific aim II. Identify NgR1 residues required to bind reovirus

Rationale: NgR1 residues in the LRR domain critical for MAI ligand binding are also proximal to neighboring σ3 molecules, as revealed by the cryo-EM model. NgR1 residues required to bind reovirus are likely also within this domain.

Hypothesis: NgR1 residues in the proximal, concave region of NgR1 are required for reovirus binding and infection. To test this hypothesis, residues proximal to σ3 molecules based on the cryo-EM reconstruction will be targeted for mutagenesis. NgR1 mutants will be assessed

for receptor expression and virus binding by flow cytometry, and infection of cells by immunofluorescence staining using a CHO gain-of-function system.

2.3 Specific aim III. Determine the role of polymorphic residue exchange between NgR1 and non-receptor family members and homologs

Rationale: NgR1 family member NgR2 is not a reovirus receptor despite sharing structural similarities to NgR1. Furthermore, human NgR1 (hNgR1) is a reovirus receptor, while murine NgR1 (mNgR1) is not. Significant amino acid sequence homology is shared between hNgR1 and non-receptor NgR2 and mNgR1, however polymorphisms exist within the proposed reovirus binding region.

Hypothesis: Exchanging NgR1-to-NgR2 residues will diminish binding and infectivity, and exchanging murine-to-human NgR1 residues will confer receptor function. To evaluate this hypothesis, a loss-of-function approach will be used to assess NgR1-to-NgR2 residue exchange and reovirus binding. Additionally, a gain-of-function approach will be used to assess murine-to-human residue exchange and reovirus binding. Reovirus binding and infection will be evaluated using a CHO gain-of-function experimental approach.

3.0 List of Abbreviations

3D: Three-dimensional

ANOVA: Analysis of variance

AMIGO3: Amphotericin-induced gene and open reading frame-3

APC: Allophycocyanin

BSL: Biosafety level

CAR: Coxsackie and adenovirus receptor

CCR5: CC chemokine receptor 5

CD4: Cluster of differentiation 4

CD46: Cluster of differentiation 46

cDNA: Circular (plasmid) DNA (deoxyribonucleic acid)

CHO: Chinese hamster ovary

CNS: Central nervous system

Cryo-EM: Cryo-electron microscopy

CXCR4: C-X-C chemokine receptor type 4

DAPI: 4',6-diamidino-2-phenylindole

DTT: dithiothreitol

EDTA: etheylenediaminetetraacetic acid

FACS: Fluorescence-activated cell sorting

FFU: Focus-forming unit

FITC: Fluorescein isothiocyanate

FSC: Forward scatter

GPI: Glycosylphosphatidylinositol

HEPES-KOH: 4-(2-hydroxyethyl)-1-piperazineethanesulfonic acid-potassium hydroxide

HIV: Human immunodeficiency virus

Ig: Immunoglobulin

JAM-A: Junction adhesion molecule-A

KOD: Thermococcus kodakaraensis polymerase

LINGO-1: Leucine-rich repeat and immunoglobulin domain-containing protein-1

LRR: Leucine-rich repeat

MAG: Myelin-associated glycoprotein

MAI: Myelin-associated inhibitor

MXRA-8: Matrix-remodeling associated protein-8

NgR1: Nogo-66 receptor 1

NgR2: Nogo-66 receptor-like 2

NgR3: Nogo-66 receptor-like 3

hNgR1: human NgR1

mNgR1: murine NgR1

OD260: Optical density (at absorbance 260)

OMgP: Oligodendrocyte myelin glycoprotein

PBS: Phosphate buffered saline

PCR: Polymerase chain reaction

PDB-ID: Protein databank identification

PirB: Paired immunoglobulin-like receptor B

SDS-PAGE: Sodium dodecyl-sulfate polyacrylamide gel electrophoresis

SEM: Standard error of the mean

siRNA: small interfering RNA (ribonucleic acid)

SSC: Side scatter

T1L: Type 1 Lang

T3D: Type 3 Dearing

V(D)J: Variable diversity joining

VLR: Variable lymphocyte receptor

WT: Wildtype

4.0 Materials and Methods

4.1 Cryo-EM, model fitting, and analysis

Purified reovirus T3SA- virions were incubated with soluble NgR1 protein (NgR1 [a.a. 1-310]-His), imbedded in vitreous ice, and imaged by cryo-EM as described (16). The three-dimensional (3D) cryo-EM reconstruction of NgR1:reovirus in complex (obtained at a final resolution of 8.9 Å) allowed fitting of protein atomic coordinates (PDB-ID *1ozn* for NgR1 (4) and *1jmu* for σ3 (5)) using the Fit in map function of UCSF Chimera (23)(version 1.16). High- and low-proximity NgR1 residues were identified in the model using the *Select zone* function in UCSF Chimera. "High-proximity" NgR1 residues were defined as residues within 5 Å of neighboring σ3 molecules, and "low-proximity" residues were defined within 5-7 Å of neighboring σ3 molecules. Buried surface area was calculated using the *Measure buried area* function in ChimeraX. Structural depictions were prepared using UCSF Chimera and ChimeraX. Accompanying experimental schematics were generated with Biorender.com.

4.2 Production of ^{35}S-labeled σ3

In vitro transcription and translation reactions were conducted using the T7 TnT® Coupled Reticulocyte Lysate system (Promega, L4610) according to the manufacturer's instructions. Reactions were supplemented with RNasin Plus RNase Inhibitor (N2611) and [^{35}S]-methionine (PerkinElmer, NEG709A500UC). Plasmid containing wildtype or mutant S4 gene cDNA was

added, and reactions were incubated at 30°C for 1 – 1.5 h. Translation reactions were terminated with 3-fold excess of stop buffer (20 mM HEPES-KOH [pH 7.4], 100 mM potassium acetate, 5 mM magnesium acetate, 5 mM EDTA, 2 mM unlabeled methionine) supplemented prior to use to contain 1 mM dithiothreitol (DTT) and 2 mM puromycin.

4.3 [^{35}S]-σ3 immunoprecipitation assays

Stop-buffer-diluted lysate expressing wildtype or mutant [^{35}S]-σ3 (28 μL) was added to 5 μg of either 10C1 antibody, a positive control antibody that binds to reovirus σ3 (24), NgR1 [a.a.1-310]-Fc protein (14), or hCAR-Fc (25). Samples (50 μL) were incubated at 4°C for 1 h rotating. Samples were subsequently incubated with 50 μL of protein G Dynabeads® (Invitrogen) at 4°C for 1 h rotating. Beads were washed seven times with Tris-buffered saline (20 mM Tris-HCl pH 7.5, 150 mM NaCl) containing 0.1% Tween-20. Samples were transferred to new tubes and diluted in 5X SDS-PAGE sample buffer containing 5% β-mercaptoethanol and incubated at 95°C for 10 min. Samples, now free of beads, were loaded into wells of pre-cast 10% Bis-Tris acrylamide gels (BioRad) and electrophoresed at 100 V for 90 min. Following SDS-PAGE, gels were fixed in 40% methanol/10% acetic acid at RT for 1 h, washed 3X with ddH2O, and dried on filter paper at 80°C for 2 h using a BioRad model 583 gel dyer. Dried gels were applied to a phosphor imaging screen for various intervals, and screens were imaged using a Cyclone Phosphor System Scanner (PerkinElmer, B431200). Bands representing [^{35}S]-methionine-labeled σ3 were quantified using Image Studio software (LI-COR, version 5.2.5).

4.4 Cells and viruses

L929 fibroblasts were maintained either in suspension or monolayer cultures in Joklik's minimal essential medium (US Biological) supplemented to contain 5% fetal bovine serum (FBS), 2 mM L-glutamine, 100 μg/mL penicillin, 100 μg/mL streptomycin, and 0.25 μg/mL amphotericin B. CHO-K1 cells (ATCC) were maintained in Ham's F12 medium (Gibco) supplemented to contain 10% FBS, 100 μg/mL penicillin, 100 μg/mL streptomycin, and 0.25 mg/mL amphotericin B.

Reovirus strain T3SA- is an engineered recombinant strain (12) that expresses nine genes of strain T1L (including the S4 gene that encodes σ3) and the S1 gene of T3 Clone 44 (26). Virus was recovered using plasmid-based reverse genetics (27, 28) and purified from infected L929 cell lysates by cesium chloride density gradient centrifugation (29). Purified virus was used in all experiments. Viral titers were determined by either particle number (estimated by spectral absorbance at 260 nm [1 OD260 = 2.1 ^{x} 1012 particles/mL]) or plaque assay using L929 cells (30).

4.5 Antibodies

Reovirus polyclonal antiserum was collected from rabbits immunized with reovirus strain T1L or T3D. Sera from T1L- and T3D-inoculated rabbits were mixed 1:1 (vol:vol) and pre-adsorbed on L929 cells to deplete non-specific antibodies. The following antibodies were used in specified assays at the indicated dilutions: anti-reovirus rabbit serum (infectivity assay – 1:1,000; flow cytometry – 1:15,000); anti-hNgR1 goat polyclonal IgG (R&D Systems; AF1208) (flow cytometry – 0.2 μg/mL); anti-hNgR2 goat polyclonal IgG (R&D Systems; AF2776) (flow

cytometry – 0.2 μg/mL); anti-mNgR1 goat polyclonal IgG (R&D Systems; AF1440) (flow cytometry – 0.2 μg/mL).

4.6 Expression plasmids

Plasmids encoding human homologs of CAR (25), NgR1 (14), NgR2 (16), or murine NgR1 (16) in pcDNA3.1 vector have been described. Plasmids containing the S4 gene open-reading frame (encoding σ3) of reovirus strain T1L (GenBank Accession: M13139.1) and T3D (GenBank Accession: HM159622.1) in pcDNA3.1+ vector have been described (16).

Site-directed mutagenesis of plasmids was conducted using custom primers (**Table 2**) and KOD Hot Start polymerase (Sigma) according to manufacturer's instructions. PCR products following mutagenesis were digested with DpnI, and DNA product size was confirmed by agarose gel electrophoresis. DNA was amplified in DH5α *E. coli* cells and purified using miniprep or midiprep kits (QIAGEN).

4.7 Transfections

CHO cells (10^5 cells/well) were seeded into 24-well tissue culture plates and cultivated overnight at 37°C in an atmosphere of 5% CO_2. Cells were transfected with cDNA using FuGene 6 (Promega, E2691) following the manufacturer's instructions and a ratio of 0.5 μg of plasmid:1.5 μL FuGene 6 in Opti-MEM (Gibco). Mock-transfected cells were incubated in Opti-MEM and

treated with FuGene 6. Cells were incubated at 37°C with 5% CO_2 for 48 h post-transfection prior to infection or flow cytometric assays.

4.8 Reovirus infection and binding

For infections, transfected CHO cells were adsorbed with reovirus diluted in PBS-/- at a multiplicity of infection (MOI) of 10 PFU/cell and incubated at 37°C for 1 h. The inoculum was removed, and cells were incubated at 37°C with 5% CO_2 in complete Ham's F12 medium. At 24 hpi, cells were washed with PBS-/- and fixed with cold methanol at -20°C for at least 30 min. Fixed cells were warmed to room temperature, washed with PBS-/-, and incubated with reovirus polyclonal antiserum diluted in 0.5% Triton X-100 in PBS-/- for 1 hr. Cells were washed with PBS-/- and incubated with Alexa Fluor® 488-labeled secondary IgG diluted in 0.5% Triton X-100 in PBS-/- for 30 min. Cells were counterstained with DAPI and imaged using a Lionheart FX automated imaging system (BioTek). Infected cells (focus-forming units or FFU) were enumerated using Gen5 software (version 3.11). FFU per field for four fields of view was calculated per well in duplicate wells.

For binding assays, transfected CHO cells were washed with PBS-/-, detached using CellStripper™ (Corning), and quenched with FACS buffer (PBS-/- supplemented to contain 2% FBS). All further incubations, washes, and pelleting were conducted on ice or at 4°C. Washes and virus incubations were conducted in PBS-/-, and antibody incubations were conducted in FACS buffer. Cells were pelleted at 500 × g for 3 min, washed, and resuspended with T3SA- (10^5 particles/cell) for 1 h. Cells were washed 3X with PBS-/- to remove unbound virus and incubated with reovirus-, NgR1-, mixed NgR1/NgR2-, or mixed hNgR1/mNgR1-specific antibodies for 1 h.

Cells were washed 3X, stained with Alexa Fluor-labelled secondary antibody for 1 h, and washed again 3X. Cells were fixed in PBS-/- supplemented to contain 1% paraformaldehyde and analyzed by flow cytometry using an LSRII flow cytometer (BD Bioscience). Results were quantified using FlowJo software (version 10).

To quantify reovirus- and receptor-bound cells, events were first gated to contain live cells using an SSC-A by FSC-A plot. Live cells were further gated using side-scatter to select events considered low in complexity or granularity, a parameter used to characterize cell health. From this population, single cells were selected using forward-scatter plots. Reovirus-bound (detected by 674-Alexa Fluor antibody) and receptor-bound (detected by 488-Alexa Fluor antibody) events were quantified and normalized to mock- and wildtype human NgR1-transfected samples using histogram plots from the final gated cell population.

4.9 Statistical analyses

Statistical tests were conducted using Prism 7 (GraphPad Software, version 9.5.1). Means of individual experiments are shown for experiments conducted five or more times. *P* values of < 0.05 were considered to be statistically significant. Descriptions of the specific tests used are provided in the figure legends.

5.0 Results

5.1 Mutations of σ3 do not ablate NgR1 binding capacity

To characterize interactions between reovirus capsid protein σ3 and NgR1, we referred to the reconstructed cryo-EM model of σ3:NgR1 engagement to identify potential amino acid residues required for binding. We rationalized that by exchanging reovirus residues in the proposed concave NgR1 binding-pocket region, we could characterize specific σ3 residues critical for NgR1 engagement. To test if we could disrupt virus binding to NgR1, we analyzed protein:protein interactions using a modified immunoprecipitation pulldown assay (summarized in **Figure 2A**). S4 expression plasmids, which encode the reovirus σ3 protein, are introduced into a coupled in vitro transcription/translation system. This system is depleted of host mRNAs and [^{35}S]-methionine, so the only nascent protein produced is radiolabeled σ3. Radiolabeled σ3-containing expression supernatants are then incubated with Protein G Dynabeads® conjugated with NgR1 or control proteins. Fc-tagged coxsackie and adenovirus receptor (CAR) is used as a negative control, as CAR does not bind σ3. Fc-containing 10C1, an antibody which specifically binds σ3, is used as a positive control for σ3 precipitation. Beads are then washed, boiled to release protein complexes, and the proteins are electrophoresed on an SDS-PAGE gel. Radiolabeled protein in the gel is visualized using phosphor imaging.

To evaluate the functionality of this assay, we first assessed NgR1 binding to σ3 proteins of two prototype reovirus strains. Experiments using atomic force microscopy to evaluate binding affinity of NgR1 to reovirus virions from T1L and T3D demonstrated comparable binding affinity between strains (16), so we suspected that polymorphisms in σ3 between these strains would not

impact NgR1 binding affinity. Expression plasmids encoding T1L and T3D σ3 were introduced into the in vitro translation system, and nascent radiolabeled σ3 proteins were assessed for their binding capacity to NgR1. As expected, no significant protein-binding differences are observed between T1L and T3D σ3 (**Figure 2B-C**). These results validate the immunoprecipitation assay, which we used as a tool to evaluate mutant σ3 binding capacity to NgR1.

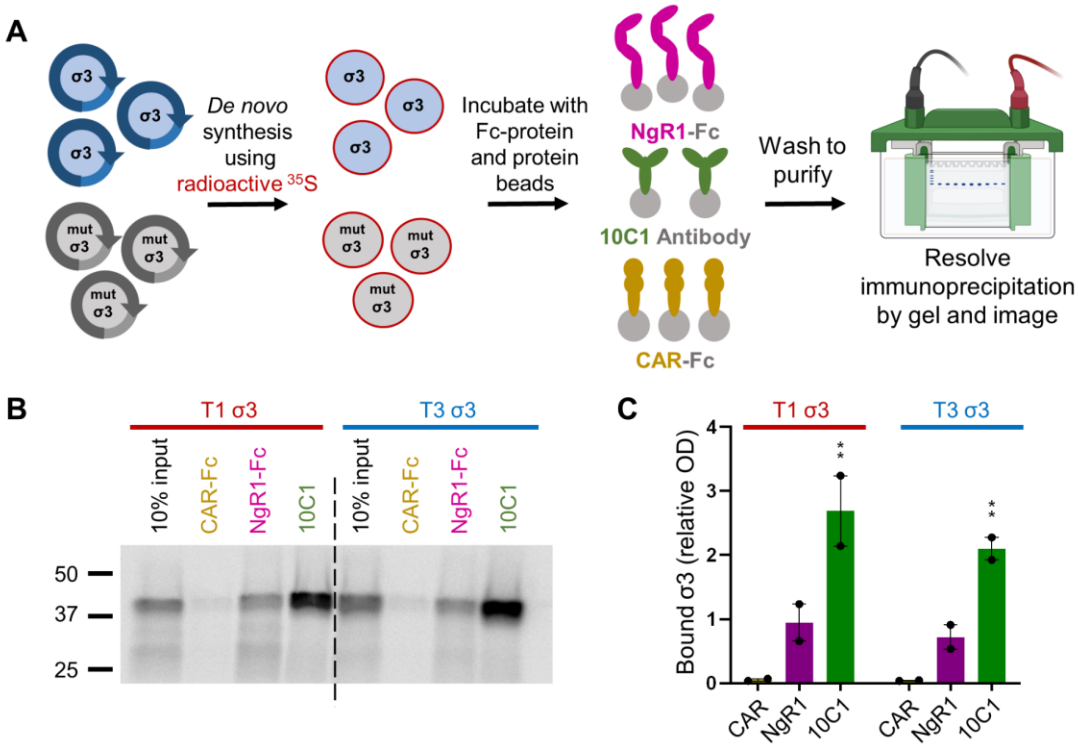

Figure 2. NgR1 binds efficiently to σ3 from two prototype reovirus strains.

(**A**) Experimental design of a modified immunoprecipitation assay to evaluate NgR1 binding to reovirus T1L, T3D, or mutant σ3 proteins. Lysates containing radiolabeled wildtype or mutant 35S-labeled σ3 were incubated with NgR1-Fc protein, σ3-specific 10C1 antibody (positive control), or CAR-Fc (negative control) conjugated to protein G Dynabeads. Samples were washed and boiled to release bound proteins. Proteins were separated by SDS-PAGE and visualized by phosphor imaging. (**B**) A representative gel comparing precipitation of σ3 from two prototype reovirus strains (T1L and T3D). (**C**) Quantification of two experimental repeats. Values that differ significantly from CAR-incubated samples by one-way ANOVA and Dunnett's test are indicated: **, $P < 0.01$.

Guided by the cryo-EM model, we identified T1L σ3 residues proximal to the concave NgR1 surface to target for mutagenesis. The surface of σ3 facing the concave NgR1 interface was chosen for mutagenesis because previous work has demonstrated the importance of this NgR1 region for ligand binding, and we hypothesized this binding interface would be critical for σ3 engagement as well. Three σ3 residues were chosen for mutagenesis (**Figure 3A**). Zoomed insets of targeted residues are shown in Figure 3B. Residue H230 extends most significantly into the proposed binding pocket and is conserved between T1L and T3D strains. We chose to exchange this residue with arginine or tryptophan, which are large and charged or aromatic, respectively. Residues D224 and S226 were also targeted for mutagenesis, and both exchanged with arginine to achieve maximal binding disruption. We hypothesized that these residues likely contribute the most to NgR1 binding, based on their sidechain orientation and proximity.

Each σ3 mutant evaluated binds NgR1 to similar levels of wildtype σ3, as shown in the representative gel image for mutant D224R (**Figure 3C**). No σ3 mutant binds CAR, the negative control, however binding to 10C1 was variable. Variability in 10C1 binding may suggest a change in mutant σ3 folding or an alteration in the epitope recognized by 10C1. Together, these data suggest σ3 binding to NgR1 may not be disrupted by single- or double-residue substitutions on one binding surface of σ3. However, these data support our hypothesis that NgR1 engages σ3 using two interfaces, and mutation of one binding surface site is likely insufficient to disrupt total receptor binding.

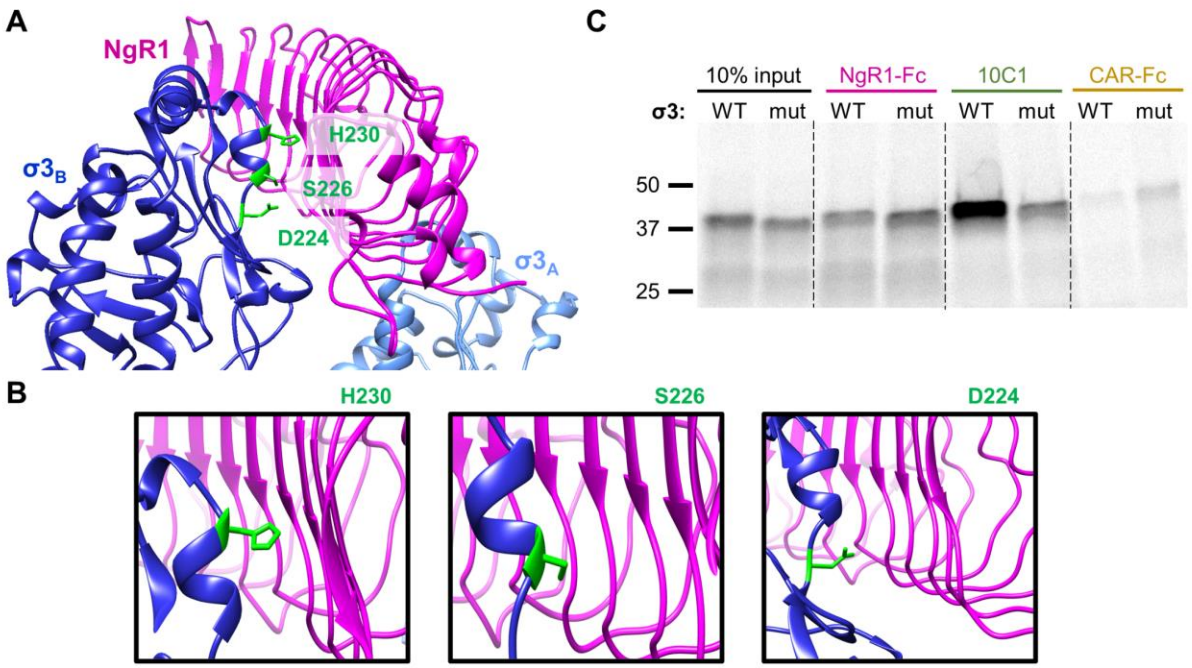

Figure 3. Substitution of σ3 residues proximal to NgR1 does not diminish NgR1 binding.

(**A**) Ribbon tracings of NgR1 engaging two σ3 protomers from the model shown in Figure 1D. Residues on the σ3 surface chosen for mutagenesis are depicted in stick format (green) on $\sigma3_B$. (**B**) Insets show each σ3 residue that was mutated for analysis. (**C**) A representative gel is shown comparing wildtype and mutant (D224R) σ3 using the modified immunoprecipitation assay.

5.2 NgR1 mutagenesis and characterization strategies

Although viral protein mutagenesis can be helpful in identifying viral residues required for host receptor engagement, this system may not be the most effective for our studies. In our reconstructed model, NgR1 is flanked by two σ3 molecules and is proposed to interact with multiple surfaces of σ3 (**Figure 1D**). Thus, we rationalized that mutagenesis of the host receptor NgR1 may be a more effective method to identify critical binding mechanisms.

To evaluate mutant NgR1 constructs for receptor expression, virus binding, and virus infection, we used a Chinese hamster ovary (CHO) cell gain-of-function system. CHO cells lack a functional reovirus receptor and are normally non-permissive to reovirus binding and infection – however, upon transfection with a cDNA encoding a functional reovirus receptor, CHO cells become permissive to virus binding and infection (31). Plasmids encoding the single NgR1 mutants are transfected into CHO cells. Cells are then assessed for receptor expression and reovirus binding via flow cytometry, or reovirus infection using immunofluorescent microscopy (summarized in **Figure 4A**). CAR is again used as a negative receptor control as it does not bind reovirus or function as a reovirus receptor.

For binding assays, cells are assessed for receptor expression and reovirus binding using flow cytometric gating strategies (**Figure 4B**). Live cells are identified from samples using SSC x FSC gates. From the live cell population, cell events are next gated to eliminate highly complex/granular cells using side-scatter plots. Single cell events are next isolated using forward-scatter plots. Once gated, the cells are then characterized for receptor expression (FITC) and virus binding (APC) using histogram plots. For infectivity assays, cells are fixed and stained using a nuclear stain (DAPI, blue) and reovirus infection (reovirus-specific polyclonal antiserum, green). Representative mock-, CAR-, and wildtype NgR1-transfected cells are pictured in Figure 4C.

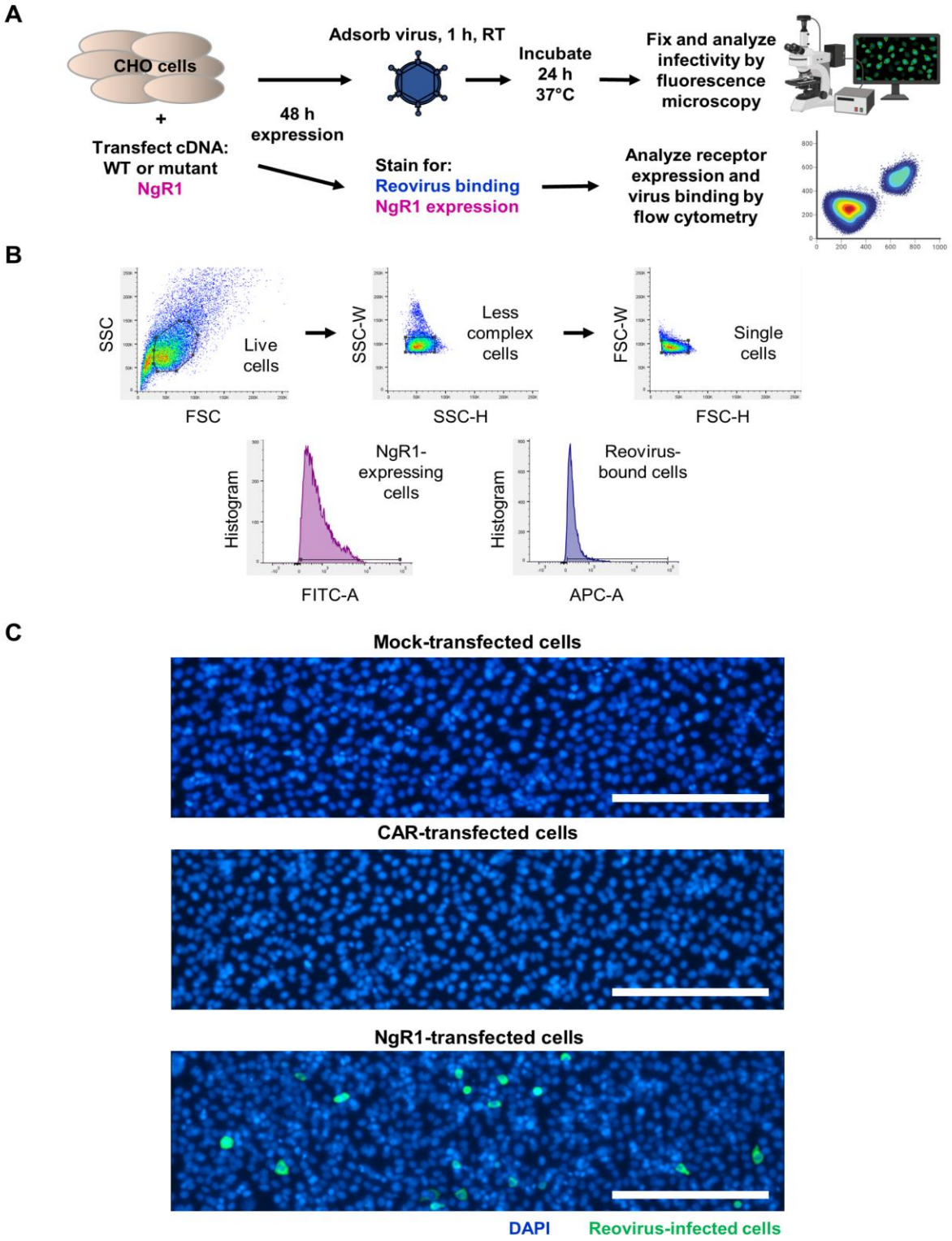

Figure 4. Experimental design for flow cytometric and fluorescence microscopy experiments.

(**A-C**) Chinese hamster ovary (CHO) cells were mock-transfected or transiently transfected with plasmids encoding wildtype NgR1, mutant NgR1, NgR2, murine NgR1, or CAR for 48 hours. Cells were stained for receptor expression using flow cytometry or adsorbed with virus, fixed, and imaged for infection using immunofluorescence microscopy. (**A**) Schematic of experimental workflow. (**B**) Representative flow cytometry profiles show the gating strategy used to capture cells detected for receptor expression or virus binding. Live cell events were first gated using SSC x FSC plots. Events low in cellular complexity were isolated using side-scatter plot gating analysis, and single-cell events were isolated using forward-scatter plot gating analysis. Single-cell events were gated using histogram plots to detect receptor expression (FITC-A) or virus binding (APC-A). (**C**) Representative immunofluorescence images. Mock-, CAR-, and NgR1-infected cells are stained with DAPI to highlight nuclei (blue) and reovirus-specific polyclonal antiserum (green). Scale bar, 200 μM.

5.3 NgR1 binds to reovirus primarily using proximal, concave residues

To characterize the precise residues of the NgR1 protein required to engage reovirus, we used a scanning mutagenesis approach guided by the cryo-EM model. To identify a panel of amino acids to target for mutagenesis, we first characterized NgR1 residues based on their proximity to σ3. Buried surface area for NgR1 residues exposed to σ3 was calculated for each NgR1 surface flanked by $\sigma3_A$ and $\sigma3_B$. This calculated surface area is inclusive of the proposed binding region used by NgR1, and is where we hypothesized critical residues are located. The buried NgR1 surface area facing the $\sigma3_A$ molecule is 142.36 Å2, and the buried surface area of the $\sigma3_B$-facing region is 793.19 Å2. Within these calculated buried surface areas, surface-exposed NgR1 residues within 5 Å of σ3 were considered high proximity and were hypothesized to have more critical binding roles than NgR1 residues in lower proximity, which range between 5 - 7 Å to σ3. Our identified mutant panel of 30 NgR1 residues in “high” and “low” proximity groups spans amino acids 119 to 258 (summarized in **Table 1**). All selected residues are within the LRR domain of NgR1, which includes amino acid residues 27 to 310, and has been previously implicated as the predominant MAI-binding domain (3).

NgR1 cDNA was mutagenized to exchange these residues with arginine, unless the native residue was arginine, in which case residues were exchanged with glutamate. Both arginine and glutamate are large and charged, and we hypothesized that substitution with one of these residues may disrupt NgR1-σ3 binding capacity. Similar approaches have been used in other virus-receptor binding studies, which successfully identified receptor residues required for virus binding. For example, this approach was used to validate host protein MXRA8 residues required for chikungunya virus binding (32) and the same strategy was used to validate JAM-A as a reovirus receptor (33). Only residues which extend away from the NgR1 protein, not residues facing the protein interior, were targeted for mutagenesis. Mutant NgR1 residues that were fully characterized are mapped onto the NgR1 molecule in **Figure 5A**. Wildtype and mutant receptor expression and virus binding are quantified by flow cytometry (**Figure 5B** and **5C**, respectively) and reovirus infection is calculated by immunofluorescence microscopy **(Figure 5D**).

Of the thirty NgR1 mutants assessed for expression at the cell surface, twenty-three mutants were confirmed to express to levels comparable to wildtype NgR1 and were subsequently pursued for virus binding and infectivity assays. We rationalized that if NgR1 mutants were not expressed or detected efficiently at the cell surface, their protein structure may be compromised or improperly folded, which could skew reovirus binding data and thus were not included for further analyses. Protein expression, virus binding, and virus infectivity data are all normalized to mock- and wildtype NgR1-transfected cells.

As hypothesized, most mutations in the high proximity group display decreased reovirus binding (**Figure 5**). Of the sixteen "high proximity" NgR1 mutants, ten mutants demonstrate significantly reduced reovirus binding capacity (determined by statistical significance). Conversely, only three of seven total "low proximity" mutants significantly diminish virus

binding. Virus binding by NgR1 mutants in the low proximity group is not completely abolished, while five high proximity mutants are rendered incapable of binding reovirus. Only one mutant in the low proximity group significantly diminishes reovirus infection, while nine mutants in the high proximity group reduce infection. Taken together, these data support the hypothesis that residues in the high proximity region are important for reovirus binding and infection.

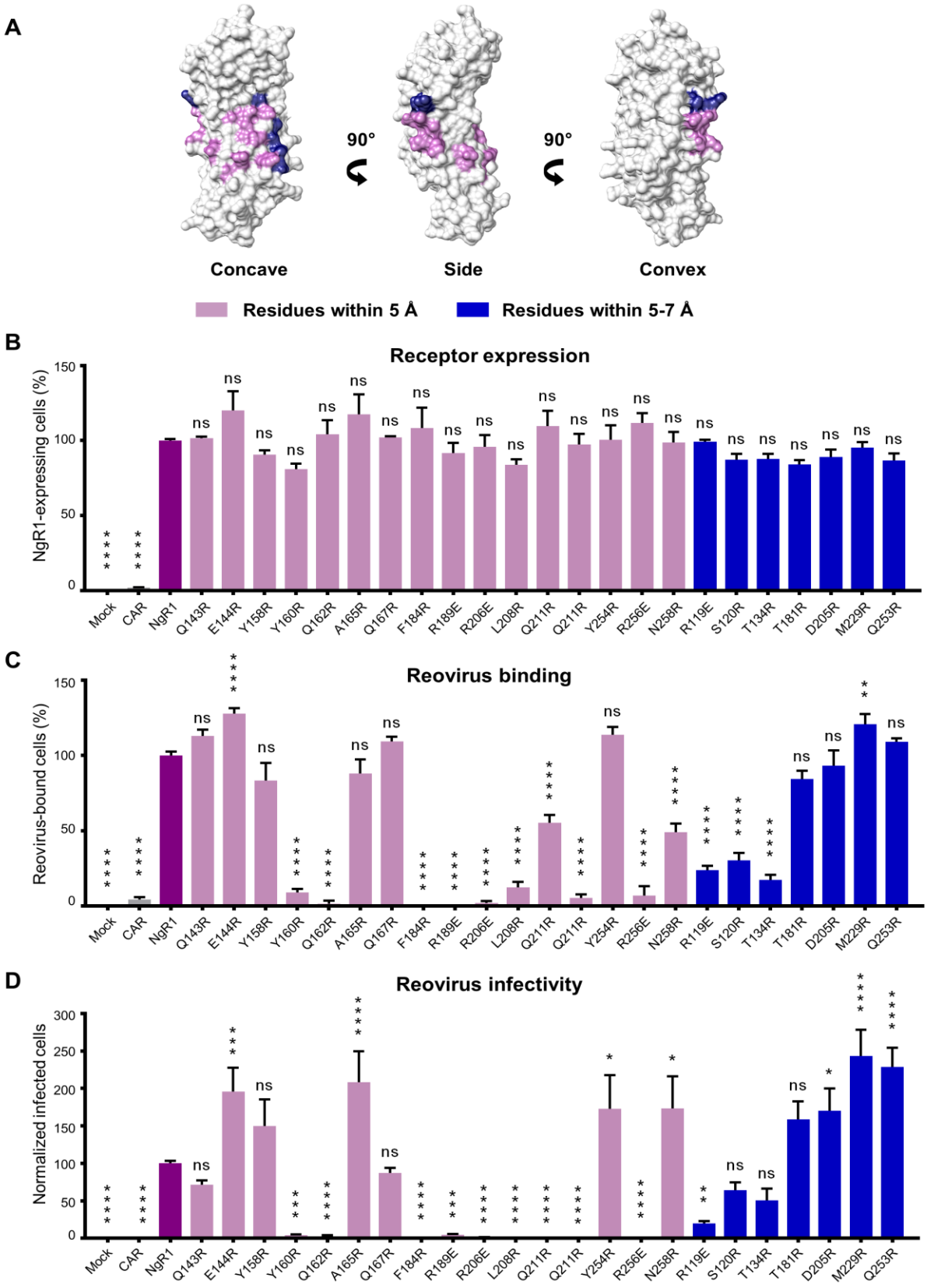

Figure 5. Many NgR1 residues proximal to σ3 are required for reovirus binding and infection.

(**A**) NgR1 residues targeted for mutagenesis are displayed on the NgR1 protein surface (*1ozn*). Selected NgR1 residues in high proximity (< 5 Å, magenta) or low proximity (5-7 Å, blue) to σ3 were exchanged with arginine or glutamate. (**B-D**) CHO cells were either mock- or transiently transfected with plasmids encoding CAR, NgR1, or mutant forms of NgR1. Transfected cells were assessed for (**B**) NgR1 expression, (**C**) reovirus binding, or (**D**) reovirus infection. Results are normalized to those obtained with wildtype NgR1- and mock-transfected cells. Error bars indicate SEM. Values that differ significantly from NgR1 by one-way ANOVA and Dunnett's test are indicated: *, $P < 0.05$; **, $P < 0.01$; ***, $P < 0.001$; ****, $P < 0.0001$; ns, not significant.

While proximity can be informative, we also wanted to evaluate the importance of residue location on the NgR1 protein. We hypothesized that NgR1 residues in the larger concave binding region may play a more important role for reovirus binding and infectivity than residues on the smaller convex surface. Based on the cryo-EM model, the σ3-facing concave NgR1 surface is much larger and contains more highly proximal residues to σ3. Furthermore, the concave NgR1 surface has shown to be critical for native NgR1 ligand engagement. Thus, data were also recategorized by their spatial position on NgR1 (**Figure 6A**). This analysis confirms many residues within the concave surface are required for virus binding and infectivity (**Figure 6B-D**). However, residue 119 on the convex surface is also important for virus binding and to a more modest extent, infection. These results suggest NgR1 engages reovirus predominantly using proximal residues within the concave region, but also utilizes residues on the convex binding surface. Encouragingly, these results support our cryo-EM model which proposes two reovirus binding sites on NgR1 and suggests that NgR1 does indeed engage σ3 using two interfaces.

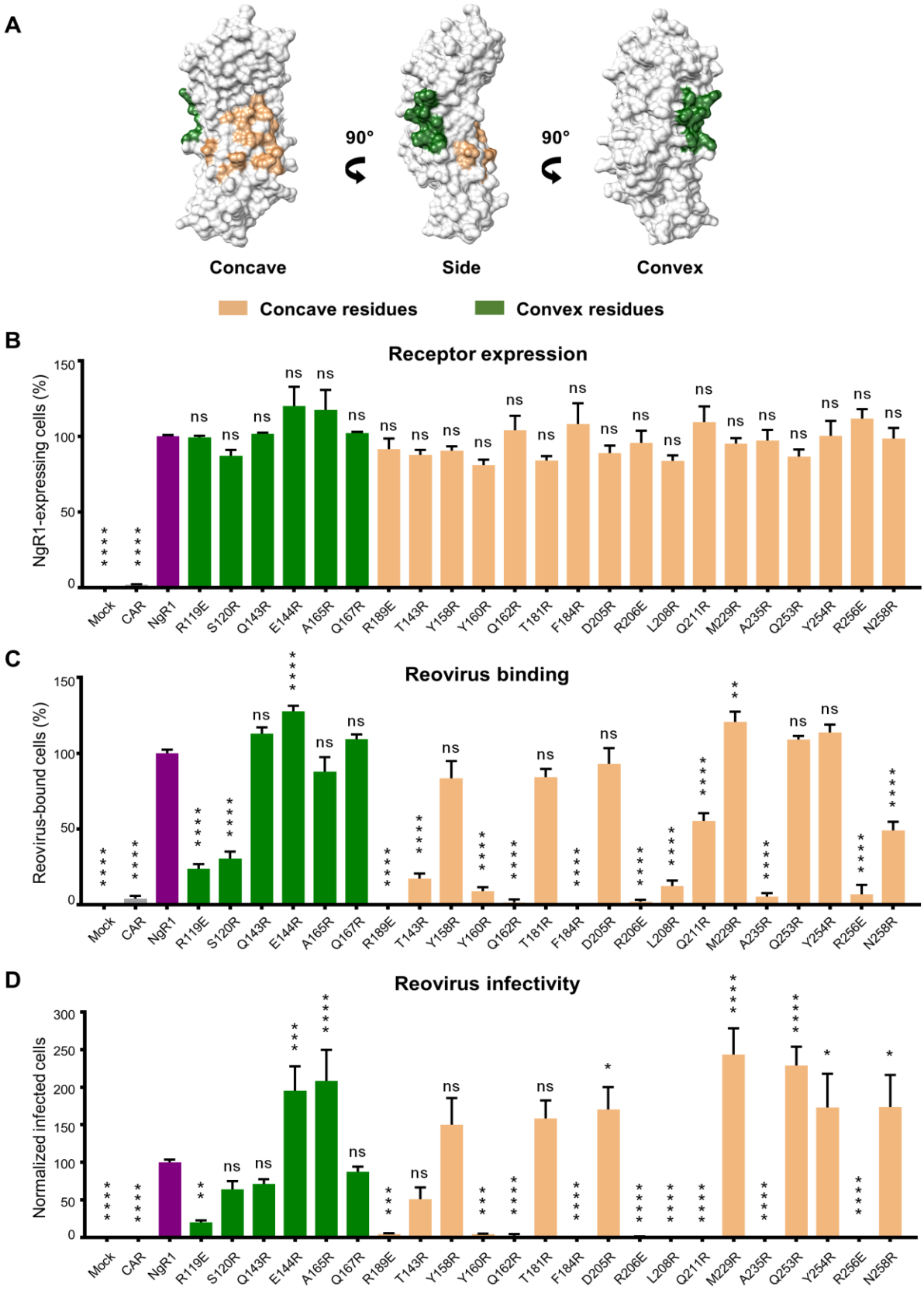

Figure 6. NgR1 residues on the concave and convex surfaces are required for reovirus binding.

(**A**) NgR1 residues targeted for mutagenesis on the convex (green) and concave surface (orange) are displayed on the NgR1 protein surface (*1ozn*). (**B-D**) CHO cells were either mock- or transiently transfected with plasmids encoding CAR, wildtype NgR1, or mutant forms of NgR1. Transfected cells were assessed for (B) NgR1 expression, (**C**) reovirus binding, or (**D**) reovirus infection. Results are normalized to those obtained with wildtype NgR1- and mock-transfected cells. Error bars indicate SEM. Values that differ significantly from NgR1 by one-way ANOVA and Dunnett's test are indicated: *, $P < 0.05$; **, $P < 0.01$; ***, $P < 0.001$; ****, $P < 0.0001$; ns, not significant.

5.4 NgR1-to-NgR2 residue exchanges do not decrease reovirus binding and infection

Although NgR1 has two known family members, NgR2 and NgR3, previous work has demonstrated that only NgR1 is capable of functioning as a reovirus receptor (however, although NgR3 expression could not be confirmed, reovirus binding was not observed, (16)). NgR1 and NgR2 both bind an MAI ligand, MAG, and share 54% amino acid sequence identity when the divergent GPI-linked tails are excluded from analysis (34). Within the LRR domain alone, NgR1 and NgR2 share 60% amino acid identity, which led us to evaluate the role of polymorphisms between NgR1 and NgR2 that could contribute to reovirus binding. Importantly in the ligand-binding concave domain, many residues are conserved, whereas multiple significant polymorphisms exist on the convex surface (**Figure 7A**). By mapping polymorphisms between NgR1 and NgR2 into our reconstructed model, we were able to visualize which residues were likely σ3 binding candidates (**Figure 7B**) and positioned to interact with neighboring reovirus proteins. We hypothesized that NgR1 residues which engage σ3 may correlate to polymorphisms between NgR2 and thus, these polymorphisms may explain the inability to bind reovirus observed with NgR2.

To test this hypothesis, we engineered three individual point mutations (highlighted in **Figure 7A and 7B**), along with double- and triple-mutant combinations of these residues. Mutations were engineered into the NgR1 cDNA backbone to effectively generate NgR1-to-NgR2

substitutions. These NgR1-to-NgR2 mutant constructs were assessed for receptor expression, virus binding, and virus infectivity in CHO cells. Each mutant construct is detected at the cell surface to levels comparable to wildtype NgR1 (**Figure 7C**). Despite adequate protein expression, neither single point mutations nor multiple mutations are able to diminish virus binding (**Figure 7D**) or infection (**Figure 7E**). These results suggest that substitution of NgR1-to-NgR2 residues at this proposed binding site is not sufficient to disrupt virus binding or infection, and suggest other residues may possibly contribute to the absence of reovirus binding observed for NgR2.

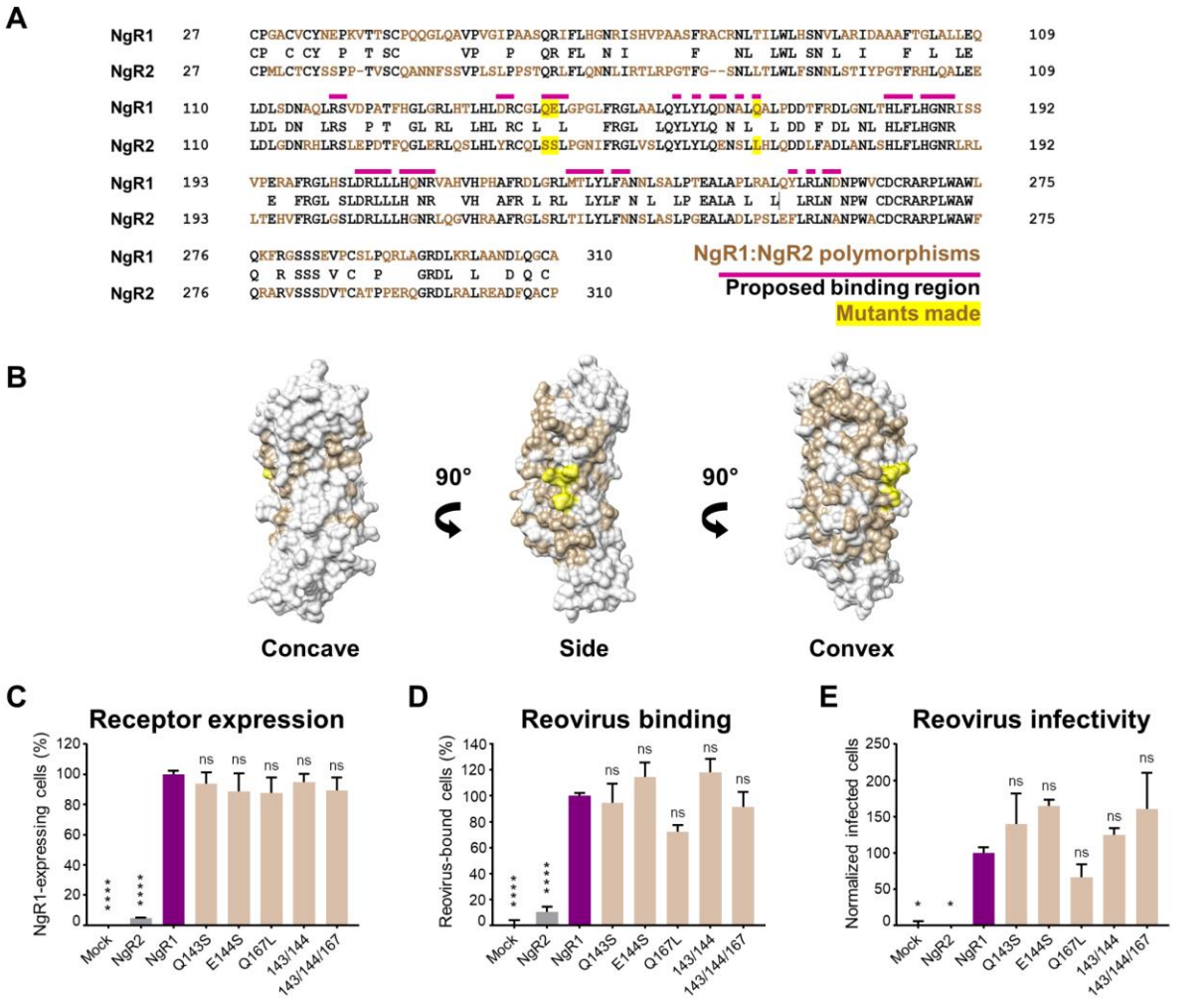

Figure 7. Exchange of selected NgR1 residues with NgR2 residues is not sufficient to ablate reovirus binding and infectivity.

(**A**) Consensus alignment of NgR1 and NgR2 LRR domains. Polymorphisms between NgR1 and NgR2 are indicated in tan, and residues targeted for mutation are highlighted in yellow. Residues within the proposed binding region (within 5 Å of neighboring σ3 molecules) are indicated with a magenta bar above the protein sequence. **(B)** Residues that vary between NgR1 and NgR2 are displayed on the NgR1 surface in tan. Residues targeted for mutagenesis are highlighted in yellow. (**C-E**) CHO cells were either mock- or transiently transfected with plasmids encoding NgR1, NgR2, or mutant forms of NgR1 incorporating NgR2 residues at the NgR1:σ3 interface. Mutants were assessed for (**C**) NgR1 expression, (**D**) reovirus binding, or (**E**) reovirus infection. Results are normalized to those obtained with wildtype NgR1- and mock-transfected cells. Error bars indicate SEM. Values that differ significantly from NgR1 by one-way ANOVA and Dunnett's test are indicated: *, $P < 0.05$; ****, $P < 0.0001$; ns, not significant.

5.5 Murine-to-human NgR1 substitutions are not sufficient to confer receptor function

While human NgR1 has been validated as a reovirus receptor, the murine homologue of NgR1 does not support reovirus binding or infection (15). Compared to moderate shared sequence identity between NgR1 and NgR2, human and murine NgR1 are more similar and share 89% protein sequence identity within the LRR domain (34). Using protein sequence alignment of human and murine NgR1, polymorphisms can be identified throughout the LRR binding domain (**Figure 8A**). These polymorphic residues (**Figure 8B**, colored on NgR1 in teal) indicate possible sites that may contribute to reovirus binding. We hypothesized that by exchanging residues in the murine NgR1 (mNgR1) backbone to human NgR1 (hNgR1), we could confer receptor function and render mNgR1 as a reovirus receptor.

Four polymorphic sites were chosen for mutagenesis using the partial sequence alignment (**Figure 8A-B**) based on their proximity to and their extension towards σ3. Using the same mutant generation and screening strategy in the mNgR1 backbone, we engineered a panel of single, double, triple, and quadruple mutants. Constructs containing multiple mutations were engineered to account for the possibility that multiple residue interactions at the protein surface may be required to promote hNgR1-like virus binding. Following transfection, all constructs are detected at the cell surface (**Figure 8C**), but no construct promotes enhanced reovirus binding (**Figure 8D**) or infection relative to hNgR1 (**Figure 8E**). These data reveal that the single- and multi-mutation constructs we designed are not sufficient to confer hNgR1-like virus binding functionality, and suggest a more complex binding relationship between virus and receptor.

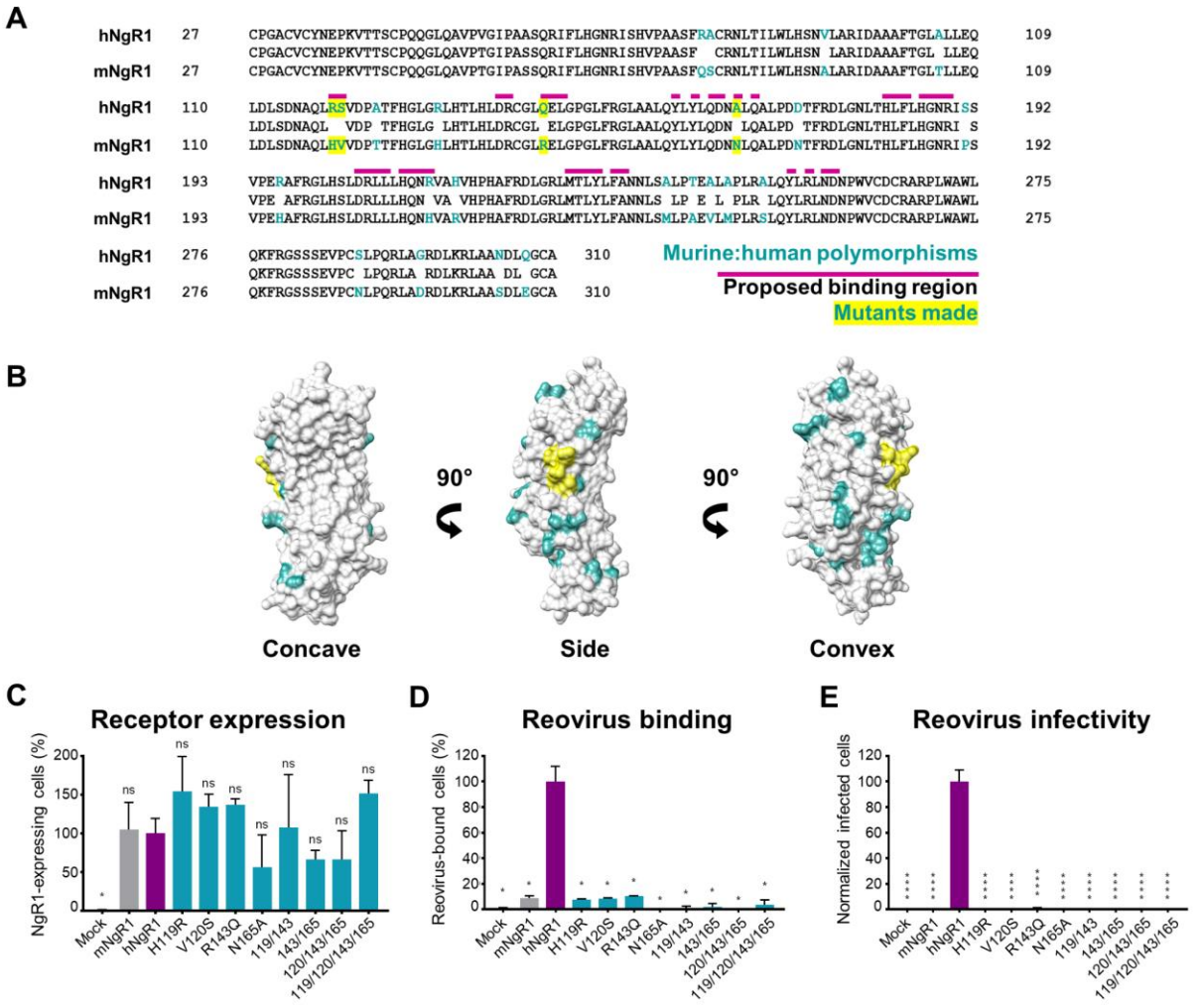

Figure 8. Exchange of selected murine NgR1 residues with human NgR1 residues is not sufficient to confer receptor function.

(**A**) Consensus alignment of human and murine NgR1 LRR domains. Polymorphisms between human and murine NgR1 are indicated in teal, and residues targeted for mutation are highlighted in yellow. Residues within the proposed binding region (within 5 Å of neighboring σ3 molecules) are indicated with a magenta bar above the protein sequence. (**B**) Polymorphic residues are mapped onto the human NgR1 surface, and residues targeted for mutation are highlighted in yellow. (**C**-**E**) CHO cells were either mock- or transiently transfected with plasmids encoding murine NgR1 (mNgR1), human NgR1 (hNgR1), or mNgR1 mutants containing selected hNgR1 residues and assessed for (**C**) NgR1 expression, (**D**) reovirus binding, and (**E**) reovirus infection. Results are normalized to those obtained with hNgR1- and mock-transfected cells. Error bars indicate SEM. Values that differ significantly from hNgR1 by student's t-test test are indicated: *, $P < 0.05$; ****, $P < 0.0001$; ns, not significant.

Table 1. Characterization of NgR1 mutants.

NgR1 mutants were characterized by expression on the cell surface, proximity to σ3, location on NgR1, capacity to diminish reovirus binding, and capacity to diminish reovirus infection. Mutant expression on the cell surface was determined by statistical comparison with expression of wildtype NgR1. Only mutants that displayed expression levels that did not differ statistically from wildtype NgR1 were pursued in subsequent reovirus binding and infectivity experiments. Proximity to neighboring σ3 molecules is depicted as "high" (within 5 Å) or "low" (5-7 Å). Location on the concave or convex NgR1 surfaces was determined using the NgR1 crystal structure. Diminished reovirus binding or infectivity was characterized as "yes" or "no" based on the results shown in Figures 5 and 6, with "yes" residues defined as mediating statistically lower binding and infectivity relative to wildtype NgR1.

NgR1 mutation	Cell surface expression	Proximity to σ3	Surface position	Diminished reovirus binding	Diminished reovirus infection
R119E	WT-LEVEL	LOW	CONVEX	YES	YES
S120R	WT-LEVEL	LOW	CONVEX	YES	NO
T134R	WT-LEVEL	LOW	CONVEX	YES	NO
Q143R	WT-LEVEL	HIGH	CONVEX	NO	NO
E144R	WT-LEVEL	HIGH	CONVEX	NO	NO
Y158R	WT-LEVEL	HIGH	CONCAVE	YES	NO
Y160R	WT-LEVEL	HIGH	CONCAVE	YES	YES
Q162R	WT-LEVEL	HIGH	CONCAVE	YES	YES
A165R	WT-LEVEL	HIGH	CONVEX	NO	NO
Q167R	WT-LEVEL	HIGH	CONVEX	NO	NO
T181R	WT-LEVEL	LOW	CONCAVE	YES	NO
F184R	WT-LEVEL	HIGH	CONCAVE	YES	YES
R189E	WT-LEVEL	HIGH	CONCAVE	YES	YES
D205R	WT-LEVEL	LOW	CONCAVE	NO	NO
R206E	WT-LEVEL	HIGH	CONCAVE	YES	YES
L208R	WT-LEVEL	HIGH	CONCAVE	YES	YES
Q211R	WT-LEVEL	HIGH	CONCAVE	YES	YES
M229R	WT-LEVEL	LOW	CONCAVE	NO	NO
A235R	WT-LEVEL	HIGH	CONCAVE	YES	YES
Q253R	WT-LEVEL	LOW	CONCAVE	NO	NO
Y254R	WT-LEVEL	HIGH	CONCAVE	NO	NO
R256E	WT-LEVEL	HIGH	CONCAVE	YES	YES
N258R	WT-LEVEL	HIGH	CONCAVE	YES	NO
L166R	UNDETECTED	N/A	N/A	N/A	N/A
H182R	UNDETECTED	N/A	N/A	N/A	N/A
H186R	UNDETECTED	N/A	N/A	N/A	N/A
H210R	UNDETECTED	N/A	N/A	N/A	N/A
T230R	UNDETECTED	N/A	N/A	N/A	N/A
Y232R	UNDETECTED	N/A	N/A	N/A	N/A
F234R	UNDETECTED	N/A	N/A	N/A	N/A

Table 2. Summary of primers used in site-directed mutagenesis of human NgR1, human NgR2, murine NgR1, and reovirus outer-capsid protein σ3.

NgR1 mutation	Forward primer (5' to 3')	Reverse primer (5' to 3')
R119E	ggcagggtccacagactcgagctgtgcattatcg	cgataatgcacagctcgagtctgtggaccctgcc
S120R	gaatgtggcagggtccactctccggagctgtgcattatc	gataatgcacagctccggagagtggaccctgccacattc
T134R	ggtgcagcctgtgtaggcggccca	tgggccgcctacacaggctgcacc
Q143R	ggcccagctcccgcaggccgcag	ctgcggcctgcgggagctgggcc
E144R	ccgggcccagccgctgcaggccgc	gcggcctgcagcggctgggcccgg
Y158R	cctgcaggtagaggcgctgcagggcagcca	tggctgccctgcagcgcctctacctgcagg
Y160R	gcgttgtcctgcaggcggaggtactgcagggc	gccctgcagtacctccgcctgcaggacaacgc
Q162R	gcagcgcgttgtcccgcaggtagaggtac	gtacctctacctgcgggacaacgcgctgc
A165R	cagtgcctgcagccggttgtcctgcagg	cctgcaggacaaccggctgcaggcactg
L166R	ggcagtgcctgccgcgcgttgtcct	aggacaacgcgcggcaggcactgcc
Q167R	atcaggcagtgcccgcagcgcgttgtc	gacaacgcgctgcgggcactgcctgat
T181R	gaagaggtgtctgaggttgcccaggtcgc	gcgacctgggcaacctcagacacctcttc
H182R	cgtgcaggaagaggcgtgtgaggttgccc	gggcaacctcacacgcctcttcctgcacg
F184R	cggttgccgtgcaggcggaggtgtgtgaggtt	aacctcacacacctccgcctgcacggcaaccg
H186R	gatgcggttgccgcgcaggaagaggtg	cacctcttcctgcgcggcaaccgcatc
R189E	gggcacgctggagatctcgttgccgtgcaggaa	ttcctgcacggcaacgagatctccagcgtgccc
D205R	gcagtaggagacggcggaggctgtgcagcc	ggctgcacagcctccgccgtctcctactgc
R206E	tctggtgcagtaggagctcgtcgaggctgtgcagc	gctgcacagcctcgacgagctcctactgcaccaga
L208R	ggttctggtgcagtcggagacggtcgagg	cctcgaccgtctccgactgcaccagaacc
H210R	cacgcggttctggcgcagtaggagacg	cgtctcctactgcgccagaaccgcgtg
Q211R	ggccacgcggttccggtgcagtaggag	ctcctactgcaccggaaccgcgtggcc
M229R	aaacagatagagtgtcctgaggcggccaaggtc	gaccttggccgcctcaggacactctatctgttt
T230R	caaacagatagagtctcatgaggcggccaaggt	accttggccgcctcatgagactctatctgtttg
Y232R	tgatagattgttggcaaacagtctgagtgtcatgaggcggccaag	cttggccgcctcatgacactcagactgtttgccaacaatctatca
F234R	cagcgctgatagattgttggctctcagatagagtgtcatgaggcg	cgcctcatgacactctatctgagagccaacaatctatcagcgctg
A235R	ctgatagattgttgcgaaacagatagagtgtcatgaggcgg	ccgcctcatgacactctatctgtttcgcaacaatctatcag
Q253R	tgagcctcaggtacctcagggcacgcaggg	ccctgcgtgccctgaggtacctgaggctca
Y254R	cgttgagcctcaggcgctgcagggcacgca	tgcgtgccctgcagcgcctgaggctcaacg
R256E	gggttgtcgttgagctccaggtactgcagggc	gccctgcagtacctggagctcaacgacaaccc
N258R	cacccaggggttgtccctgagcctcaggtact	agtacctgaggctcagggacaacccctgggtg

NgR1-to-NgR2 mutation	Forward primer (5' to 3')	Reverse primer (5' to 3')
Q143S	ccgggcccagctcgctcaggccgcagcgg	ccgctgcggcctgagcgagctgggcccgg
E144S	gccccgggcccaggctctgcaggccgcag	ctgcggcctgcagagcctgggcccggggc
Q167L	atcaggcagtgccagcagcgcgttgtc	gacaacgcgctgctggcactgcctgat
Q143S/E144S	acagccccgggcccaggctgctcaggccgcagcggtcc	ggaccgctgcggcctgagcagcctgggcccggggctgt

Murine-to-human NgR1 mutation	Forward primer (5' to 3')	Reverse primer (5' to 3')
H119R	cgtggtagggtccacgacccgaagctgtgcattatcac	gtgataatgcacagcttcgggtcgtggaccctaccacg
V120S	tggtagggtccacgctatgaagctgtgcattatcactaaga	tcttagtgataatgcacagcttcatagcgtggaccctacca
R143Q	ggacccagctcctgcaggccacatc	gatgtggcctgcaggagctgggtcc
N165A	tcagggagtgcctgcagagcgttgtcttgtaggtagag	ctctacctacaagacaacgctctgcaggcactccctga

σ3/S4 mutation	Forward primer (5' to 3')	Reverse primer (5' to 3')
H230W	gcacggcccttcgatggatcccactctaactcagagtaatcgt	acgattactctgagttagagtgggatccatcgaagggccgtgc
H230R	ggcccttcgatggatcacgctctaactcagagtaa	ttactcgagttagagcgtgatccatcgaagggcc
D224R	catgctctaactcagagtaacggtaaaccatcacaccccatt	aatggggtgtgatggtttaccgttactctgagttagagcatg
S226R	gatggatcatgctctaactcacggtaatcgtaaaccatcacacc	ggtgtgatggtttacgattaccgtgagttagagcatgatccatc

6.0 Discussion

To enter cells, viruses engage attachment factors, entry receptors, or a combination of these host molecules using one or more viral proteins. These specific interactions between virus and cell dictate which cells become infected within the host and how the virus spreads throughout and between hosts. Reovirus engages multiple host receptors and uses a variety of structural proteins to bind these molecules. Using multiple capsid proteins to bind an array of host receptors promotes reovirus entry and replication in many cell types, including cells in the CNS. Other viruses also are capable of using multiple capsid proteins to bind host attachment factors and entry receptors. For example, adenovirus uses fiber, penton, and hexon capsid proteins to engage host receptors including CAR (35), sialylated glycans (36), and CD46 to enter cells (20). In this study, we characterized interactions between reovirus capsid protein σ3 and host receptor NgR1 to elucidate the molecular interactions required for viral infection.

To characterize the newly identified binding interactions of reovirus and NgR1, we first evaluated residues of the reovirus σ3 protein within the proposed NgR1-binding domain for the capacity to influence binding to NgR1. We found that σ3 residue exchange within this domain was not sufficient to diminish NgR1 binding (**Figure 3C**), which supports our proposed model of reovirus in complex with NgR1. We chose to only alter one surface of σ3, although our model suggests NgR1 engagement by multiple σ3 surfaces (**Figure 1D**). Although residue exchange on one σ3 surface was not sufficient to disrupt NgR1 binding, it is possible that residue exchange on all NgR1-binding surfaces of σ3 simultaneously would diminish NgR1 engagement. To test this hypothesis, residue exchange within multiple σ3 surfaces proposed to interact with NgR1 would need to be characterized using NgR1-binding assays.

We next evaluated residues in NgR1 required for binding to reovirus and identified several NgR1 residues required for both binding and infection (**Figure 5**). These critical residues are within the MAI ligand-binding region of NgR1, suggesting redundancy in the use of this domain to bind other ligands (including viral capsid components). Importantly, residues required for reovirus binding are present on both the concave and convex surfaces of NgR1 (**Figure 6**). Use of both NgR1 surfaces to bind reovirus validates our cryo-EM model of reovirus engagement and supports our hypothesis that NgR1 binds reovirus by bridging two σ3 molecules. These results also suggest that reovirus binds a host receptor using a canyon formed by σ3 capsid proteins, analogous to the receptor-binding canyons in picornaviruses (19). This receptor-binding strategy has not been previously described for reovirus.

We conducted additional experiments to evaluate whether exchange of polymorphic residues between human NgR1 and non-receptor family members and homologs, NgR2 and murine NgR1, could influence reovirus binding. Loss-of-function residue exchange using NgR1-to-NgR2 constructs was not sufficient to diminish reovirus binding and infection (**Figure 7**). Additionally, gain-of-function residue exchange using murine-to-human NgR1 constructs was not sufficient to confer reovirus receptor functionality (**Figure 8**). Although we did not evaluate every possible residue exchange between NgR1 proteins, our results suggest a more complex binding relationship between reovirus and NgR1 that is not dependent on single residues alone.

Reovirus binds human NgR1 using multiple σ3 surfaces, engages multiple NgR1 domains, and may even bind other NgR1-interacting partners specific only to human NgR1. A co-receptor for human NgR1 may be required for reovirus entry into host cells following initial NgR1 binding, analogous to the requirements for co-receptors CCR5 or CXCR4 for HIV cell entry following CD4 binding (37, 38). Multiple co-receptors for NgR1 have been identified and are used to engage MAI

ligands in the CNS and promote downstream signaling (17). Known NgR1 co-receptors include p75 (39), LINGO-1 (40), and AMIGO3 (41). If these co-receptors also are required for reovirus binding or cell entry, they could be evaluated using protein-binding assays to define possible functions as co-receptors for reovirus.

While most humans experience one or more reovirus infections by adolescence, disease is rare (8, 9). However, reovirus causes significant and sometimes lethal disease in newborn mice (42, 43). Species-specific host factors that contribute to differences in reovirus virulence have not been identified, but the age of the host is a major contributor (44). However, understanding the different roles of receptor homologs in mice and humans contributes to our knowledge of reovirus-mediated disease. Murine NgR1 is not a reovirus receptor, while human NgR1 confers this function. Therefore, we hypothesize that another receptor is used by reovirus to bind and enter murine neurons. Consistent with this hypothesis, we recently identified the murine homolog of paired immunoglobulin receptor B (PirB) as a neural receptor that promotes reovirus binding and entry (45). Remarkably, PirB displays partially overlapping expression with NgR1, shares native MAI ligands with NgR1, and is required for full reovirus neurovirulence in mice. Furthermore, while murine PirB is a functional reovirus receptor, the human homolog of PirB does not bind reovirus. Although NgR1 and PirB are structurally dissimilar, we hypothesize that each functions to allow reovirus infection of CNS neurons in humans (NgR1) or mice (PirB). Since reovirus infects most mammalian species, it is not surprising that reovirus uses many receptors to infect mammalian hosts. Understanding how NgR1 and PirB function as reovirus receptors in a variety of host species may reveal an evolutionary bridge between these proteins that has been exploited by reovirus to infect a broad range of mammals.

The main NgR1 structural motif, the leucine-rich repeat (LRR), is widely used in plants and animals and often contributes to innate immune functions. For example, a large group of LRR proteins in plants, referred to as R proteins, protect against invading pathogens by recognizing pathogen-associated effectors that dampen innate immune responses (46). In animals, Toll-like receptors are LRR proteins that bind pathogen-associated molecular patterns, such as viral dsRNA or bacterial lipopolysaccharide, to activate innate immune signaling. LRR proteins also have been implicated in some types of adaptive immunity. Jawed vertebrates, or gnathostomes, evolved to use V(D)J recombination to produce a repertoire of lymphocyte receptors based on the immunoglobulin (Ig) fold to recognize pathogens or pathogen components (47). Conversely, jawless vertebrates, or agnathans, generate adaptive immune receptors using an alternative mechanism. Modular LRR domains are reorganized by somatic rearrangement to form a repertoire of variable lymphocyte receptors (VLRs) used as adaptive immune mediators to protect against invading pathogens (48). This alternative VLR method yields an equivalent repertoire of antigen receptors as V(D)J recombination and Ig domains, which function in a manner similar to lymphocyte receptors to bind pathogens using the LRR motif (49). Surviving agnathan species, hagfish and lampreys, are the only known vertebrates to employ the VLR mechanism of adaptive lymphocyte receptor function. Thus, intricate relationships between LRR proteins and pathogens have co-evolved for hundreds of millions of years. Therefore, it is not surprising that viruses can recognize the conserved LRR motifs in proteins and, furthermore, can bind these motifs to enter cells.

In the evolutionary arms race between pathogen and host, viruses (including reovirus) have adapted to bind pathogen receptors to establish infection rather than initiate clearance by the adaptive immune response. Numerous viruses engage receptors with shared adaptive immune

structural motifs, such as the Ig fold (50). For example, coxsackie virus and adenovirus bind CAR, which contains two Ig-like domains (51), herpes simplex virus binds nectin proteins, which contain three Ig-like domains (52, 53), and reovirus σ1 binds JAM-A, which contains two Ig-like domains (25). As Ig domain-containing proteins are widely used as viral receptors, it was not surprising to find another class of adaptive immunity motif-containing proteins that functions as a viral receptor. LRR motif-containing proteins, such as NgR1, also may be used as receptors for other pathogens, although we are not aware of examples in addition to NgR1.

Reovirus receptor NgR1 is predominantly expressed by neurons. Following binding to its natural ligands in the CNS, NgR1 inhibits axonal outgrowth (54-56). Axonal outgrowth inhibition is a critical function in neuron maturation in developing mammals and disrupts neuronal repair after injury. Neuron damage caused by viral infection can lead to serious outcomes such as encephalitis, paralysis, behavioral changes, and even death (57). NgR1 expression by neurons is increased following injury (58), which may provide a feed-forward mechanism of viral infection and damage. Understanding how viruses enter such highly protected cells can help inform therapeutic approaches to mitigate virus-induced damage in neurons.

Reovirus is one of many pathogens that infect neurons. Rabies virus first infects peripheral neurons and disseminates to the CNS by traversing synapses to cause fatal neurological disease in a variety of mammalian hosts (59, 60). Herpes simplex virus also invades the CNS by first traversing peripheral neurons and can establish latency in neurons for extended intervals before reactivating (61). Zika virus invades neurons to cause microcephaly in newborn infants (62, 63). Although these viruses differ in their genome characteristics and replication cycle, are from distinct viral families, follow different routes of infection, and lead to different symptoms, they cause significant disease by infecting neurons in their respective hosts. Therefore, it is crucial to

understand mechanisms and receptors used by neurotropic viruses to guide therapeutic approaches. Reovirus is a powerful experimental system to answer these questions, as it is a neurotropic virus that causes significant disease in mice. Experiments with reovirus can be conducted using relatively low biosafety conditions, which is less expensive and more accessible than the biocontainment requirements for other neurotropic viruses. For example, reovirus experiments can be conducted using BSL2 conditions, whereas rabies virus experiments require BSL3 containment. Reovirus also is easily cultivated, amenable to genetic manipulation using reverse genetics, can be purified in large quantities for biochemical studies, and readily infects laboratory mice. Thus, reovirus as a model system to study neurotropic disease is valuable in the context of public health, as we can apply insights gained from reovirus to develop therapeutic interventions for other pathogens.

In addition to providing an excellent model system to study viral neuropathogenesis, reovirus also is a pathogen of concern for pandemic potential. Reovirus shares many attributes of other pandemic-causing viruses such as coronavirus and influenza virus. Reovirus contains a segmented genome, which allows gene segment reassortment and the capacity to rapidly exchange genetic traits. Virtually all mammals are hosts for reovirus, which provides an ample reservoir for reassortment and emergence of new viral strains. Our study robustly contributes to an understanding of the biochemical mechanisms used by reovirus to infect NgR1-expressing cells. Given the possibility of emergence of more virulent reovirus strains, expanding our knowledge of reovirus binding and infection may contribute to prevention and treatment strategies should more virulent strains emerge.

Bibliography

1. Zhang X, Ji Y, Zhang L, Harrison SC, Marinescu DC, Nibert ML, Baker TS. 2005. Features of reovirus outer capsid protein m1 revealed by electron cryomicroscopy and image reconstruction of the virion at 7.0 Å resolution. Structure 13:1545-57.
2. Dietrich MH, Ogden KM, Long JM, Ebenhoch R, Thor A, Dermody TS, Stehle T. 2018. Structural and functional features of the reovirus s1 tail. J Virol 92:e00336-18.
3. Lauren J, Hu F, Chin J, Liao J, Airaksinen MS, Strittmatter SM. 2007. Characterization of myelin ligand complexes with neuronal Nogo-66 receptor family members. J Biol Chem 282:5715-25.
4. He XL, Bazan JF, McDermott G, Park JB, Wang K, Tessier-Lavigne M, He Z, Garcia KC. 2003. Structure of the Nogo receptor ectodomain: a recognition module implicated in myelin inhibition. Neuron 38:177-85.
5. Liemann S, Chandran K, Baker TS, Nibert ML, Harrison SC. 2002. Structure of the reovirus membrane-penetration protein, m1, in a complex with its protector protein, s3. Cell 108:283-95.
6. Tunkel AR, Glaser CA, Bloch KC, Sejvar JJ, Marra CM, Roos KL, Hartman BJ, Kaplan SL, Scheld WM, Whitley RJ. 2008. The management of encephalitis: clinical practice guidelines by the Infectious Diseases Society of America. Clin Infect Dis 47:303-27.
7. Kneen R, Michael BD, Menson E, Mehta B, Easton A, Hemingway C, Klapper PE, Vincent A, Lim M, Carrol E, Solomon T. 2012. Management of suspected viral encephalitis in children - Association of British Neurologists and British Paediatric Allergy, Immunology and Infection Group national guidelines. J Infect 64:449-77.
8. Dermody TS, Parker JS, Sherry B. 2013. Orthoreoviruses, p 1304-1346. *In* Knipe DM, Howley PM (ed), Fields Virology, 6th ed, vol 2. Lippincott Williams & Wilkins, Philadelphia.
9. Tai JH, Williams JV, Edwards KM, Wright PF, Crowe JE, Jr., Dermody TS. 2005. Prevalence of reovirus-specific antibodies in young children in Nashville, Tennessee. J Infect Dis 191:1221-4.
10. Weiner HL, Drayna D, Averill DR, Jr., Fields BN. 1977. Molecular basis of reovirus virulence: role of the S1 gene. Proc Natl Acad Sci U S A 74:5744-8.
11. Chappell JD, Duong JL, Wright BW, Dermody TS. 2000. Identification of carbohydrate-binding domains in the attachment proteins of type 1 and type 3 reoviruses. J Virol 74:8472-9.
12. Sutherland DM, Aravamudhan P, Dietrich MH, Stehle T, Dermody TS. 2018. Reovirus neurotropism and virulence are dictated by sequences in the head domain of the viral attachment protein. J Virol 92:e00974-18.

13. Antar AAR, Konopka JL, Campbell JA, Henry RA, Perdigoto AL, Carter BD, Pozzi A, Abel TW, Dermody TS. 2009. Junctional adhesion molecule-A is required for hematogenous dissemination of reovirus. Cell Host Microbe 5:59-71.

14. Konopka-Anstadt JL, Mainou BA, Sutherland DM, Sekine Y, Strittmatter SM, Dermody TS. 2014. The Nogo receptor NgR1 mediates infection by mammalian reovirus. Cell Host Microbe 15:681-91.

15. Aravamudhan P, Guzman-Cardozo, C, Urbanek, K, Welsh, OL, Konopka-Anstadt, JL, Sutherland, DM, and Dermody, TS. 2021. The murine neuronal receptor NgR1 is dispensable for reovirus pathogenesis. J Virol 96:e00055-22.

16. Sutherland DM, Strebl M, Koehler M, Welsh OL, Yu X, Hu L, Dos Santos Natividade R, Knowlton JJ, Taylor GM, Moreno RA, Wörz P, Lonergan ZR, Aravamudhan P, Guzman-Cardozo C, Kour S, Pandey UB, Alsteens D, Wang Z, Prasad BVV, Stehle T, Dermody TS. 2023. NgR1 binding to reovirus reveals an unusual bivalent interaction and a new viral attachment protein. Proc Natl Acad Sci U S A 120:e2219404120.

17. McGee AW, Strittmatter SM. 2003. The Nogo-66 receptor: focusing myelin inhibition of axon regeneration. Trends Neurosci 26:193-8.

18. Xie F, Zheng B. 2008. White matter inhibitors in CNS axon regeneration failure. Exp Neurol 209:302-12.

19. Rossmann MG. 1989. The canyon hypothesis. Hiding the host cell receptor attachment site on a viral surface from immune surveillance. J Biol Chem 264:14587-90.

20. Persson BD, John L, Rafie K, Strebl M, Frängsmyr L, Ballmann MZ, Mindler K, Havenga M, Lemckert A, Stehle T, Carlson LA, Arnberg N. 2021. Human species D adenovirus hexon capsid protein mediates cell entry through a direct interaction with CD46. Proc Natl Acad Sci U S A 118.

21. Xing L, Casasnovas JM, Cheng RH. 2003. Structural analysis of human rhinovirus complexed with ICAM-1 reveals the dynamics of receptor-mediated virus uncoating. J Virol 77:6101-7.

22. Olson NH, Kolatkar PR, Oliveira MA, Cheng RH, Greve JM, McClelland A, Baker TS, Rossmann MG. 1993. Structure of a human rhinovirus complexed with its receptor molecule. Proc Natl Acad Sci U S A 90:507-11.

23. Pettersen EF, Goddard TD, Huang CC, Couch GS, Greenblatt DM, Meng EC, Ferrin TE. 2004. UCSF chimera-a visualization system for exploratory research and analysis. J Comput Chem 25:1605-12.

24. Virgin HW, IV, Mann MA, Fields BN, Tyler KL. 1991. Monoclonal antibodies to reovirus reveal structure/function relationships between capsid proteins and genetics of susceptibility to antibody action. J Virol 65:6772-6781.

25. Barton ES, Forrest JC, Connolly JL, Chappell JD, Liu Y, Schnell FJ, Nusrat A, Parkos CA, Dermody TS. 2001. Junction adhesion molecule is a receptor for reovirus. Cell 104:441-51.

26. Chappell JD, Gunn VL, Wetzel JD, Baer GS, Dermody TS. 1997. Mutations in type 3 reovirus that determine binding to sialic acid are contained in the fibrous tail domain of viral attachment protein s1. J Virol 71:1834-1841.

27. Kobayashi T, Antar AA, Boehme KW, Danthi P, Eby EA, Guglielmi KM, Holm GH, Johnson EM, Maginnis MS, Naik S, Skelton WB, Wetzel JD, Wilson GJ, Chappell JD, Dermody TS. 2007. A plasmid-based reverse genetics system for animal double-stranded RNA viruses. Cell Host Microbe 1:147-57.

28. Kobayashi T, Ooms LS, Ikizler M, Chappell JD, Dermody TS. 2010. An improved reverse genetics system for mammalian orthoreoviruses. Virology 398:194-200.

29. Berard A, Coombs KM. 2009. Mammalian reoviruses: propagation, quantification, and storage. Curr Protoc Microbiol Chapter 15:Unit15C 1.

30. Virgin HW, Bassel-Duby R, Fields BN, Tyler KL. 1988. Antibody protects against lethal infection with the neurally spreading reovirus type 3 (Dearing). J Virol 62:4594-604.

31. Forrest JC, Campbell JA, Schelling P, Stehle T, Dermody TS. 2003. Structure-function analysis of reovirus binding to junctional adhesion molecule 1. Implications for the mechanism of reovirus attachment. J Biol Chem 278:48434-44.

32. Zhang R, Kim AS, Fox JM, Nair S, Basore K, Klimstra WB, Rimkunas R, Fong RH, Lin H, Poddar S, Crowe JE, Jr., Doranz BJ, Fremont DH, Diamond MS. 2018. Mxra8 is a receptor for multiple arthritogenic alphaviruses. Nature doi:10.1038/s41586-018-0121-3.

33. Guglielmi KM, Kirchner E, Holm GH, Stehle T, Dermody TS. 2007. Reovirus binding determinants in junctional adhesion molecule-A. J Biol Chem 282:17930-40.

34. Lauren J, Airaksinen MS, Saarma M, Timmusk T. 2003. Two novel mammalian Nogo receptor homologs differentially expressed in the central and peripheral nervous systems. Mol Cell Neurosci 24:581-94.

35. He Y, Chipman PR, Howitt J, Bator CM, Whitt MA, Baker TS, Kuhn RJ, Anderson CW, Freimuth P, Rossmann MG. 2001. Interaction of coxsackievirus B3 with the full length coxsackievirus-adenovirus receptor. Nat Struct Biol 8:874-8.

36. Chiu CY, Mathias P, Nemerow GR, Stewart PL. 1999. Structure of adenovirus complexed with its internalization receptor, avb5 integrin. J Virol 73:6759-6768.

37. Feng Y, Broder CC, Kennedy PE, Berger EA. 1996. HIV-1 entry cofactor: functional cDNA cloning of a seven-transmembrane, G protein-coupled receptor. Science 272:872-7.

38. Dragic T, Litwin V, Allaway GP, Martin SR, Huang YX, Nagashima KA, Cayanan C, Maddon PJ, Koup RA, Moore JP, Paxton WA. 1996. HIV-1 entry into CD4(+) cells is mediated by the chemokine receptor CC-CKR-5. Nature 381:667-673.

39. Wang KC, Kim JA, Sivasankaran R, Segal R, He Z. 2002. P75 interacts with the Nogo receptor as a co-receptor for Nogo, MAG and OMgp. Nature 420:74-8.

40. Mi S, Lee X, Shao Z, Thill G, Ji B, Relton J, Levesque M, Allaire N, Perrin S, Sands B, Crowell T, Cate RL, McCoy JM, Pepinsky RB. 2004. LINGO-1 is a component of the Nogo-66 receptor/p75 signaling complex. Nat Neurosci 7:221-8.

41. Ahmed Z, Douglas MR, John G, Berry M, Logan A. 2013. AMIGO3 is an NgR1/p75 co-receptor signalling axon growth inhibition in the acute phase of adult central nervous system injury. PLoS One 8:e61878.

42. Masters C, Alpers M, Kakulas B. 1977. Pathogenesis of reovirus type 1 hydrocephalus in mice. Significance of aqueductal changes. Arch Neurol 34:18-28.

43. Tyler KL, McPhee DA, Fields BN. 1986. Distinct pathways of viral spread in the host determined by reovirus S1 gene segment. Science 233:770-4.

44. Wu AG, Pruijssers AJ, Brown JJ, Stencel-Baerenwald JE, Sutherland DM, Iskarpatyoti JA, Dermody TS. 2018. Age-dependent susceptibility to reovirus encephalitis in mice is influenced by maturation of the type-I interferon response. Pediatr Res 83:1057-66.

45. Shang P, Simpson JD, Taylor GM, Sutherland DM, Welsh OL, Aravamudhan P, Natividade RDS, Schwab K, Michel JJ, Poholek AC, Wu Y, Rajasundaram D, Koehler M, Alsteens D, Dermody TS. 2023. Paired immunoglobulin-like receptor B is an entry receptor for mammalian orthoreovirus. Nat Commun 14:2615.

46. Zipfel C. 2008. Pattern-recognition receptors in plant innate immunity. Curr Opin Immunol 20:10-6.

47. Murphy K, Travers P, Walport M, Janeway C. 2012. Janeway's immunobiology, 8th ed. Garland Science, New York.

48. Buchmann K. 2014. Evolution of innate immunity: clues from invertebrates via fish to mammals. Front Immunol 5:459.

49. Alder MN, Rogozin IB, Iyer LM, Glazko GV, Cooper MD, Pancer Z. 2005. Diversity and function of adaptive immune receptors in a jawless vertebrate. Science 310:1970-3.

50. Dermody TS, Kirchner E, Guglielmi KM, Stehle T. 2009. Immunoglobulin superfamily virus receptors and the evolution of adaptive immunity. PLoS Pathog 5:e1000481.

51. Bergelson JM, Cunningham JA, Droguett G, Kurt-Jones EA, Krithivas A, Hong JS, Horwitz MS, Crowell RL, Finberg RW. 1997. Isolation of a common receptor for Coxsackie B viruses and adenoviruses 2 and 5. Science 275:1320-3.

52. Geraghty RJ, Krummenacher C, Cohen GH, Eisenberg RJ, Spear PG. 1998. Entry of alphaherpesviruses mediated by poliovirus receptor-related protein 1 and poliovirus receptor. Science 280:1618-20.

53. Warner MS, Geraghty RJ, Martinez WM, Montgomery RI, Whitbeck JC, Xu R, Eisenberg RJ, Cohen GH, Spear PG. 1998. A cell surface protein with herpesvirus entry activity (HveB) confers susceptibility to infection by mutants of herpes simplex virus type 1, herpes simplex virus type 2, and pseudorabies virus. Virology 246:179-89.

54. Fournier AE, GrandPre T, Strittmatter SM. 2001. Identification of a receptor mediating Nogo-66 inhibition of axonal regeneration. Nature 409:341-6.

55. Domeniconi M, Cao Z, Spencer T, Sivasankaran R, Wang K, Nikulina E, Kimura N, Cai H, Deng K, Gao Y, He Z, Filbin M. 2002. Myelin-associated glycoprotein interacts with the Nogo66 receptor to inhibit neurite outgrowth. Neuron 35:283-90.

56. Wang KC, Koprivica V, Kim JA, Sivasankaran R, Guo Y, Neve RL, He Z. 2002. Oligodendrocyte-myelin glycoprotein is a Nogo receptor ligand that inhibits neurite outgrowth. Nature 417:941-4.

57. Berth SH, Leopold PL, Morfini GN. 2009. Virus-induced neuronal dysfunction and degeneration. Front Biosci (Landmark Ed) 14:5239-59.

58. Ukai J, Imagama S, Ohgomori T, Ito Z, Ando K, Ishiguro N, Kadomatsu K. 2016. Nogo receptor 1 is expressed in both primary cultured glial cells and neurons. Nagoya J Med Sci 78:303-11.

59. Bauer A, Nolden T, Schröter J, Römer-Oberdörfer A, Gluska S, Perlson E, Finke S. 2014. Anterograde glycoprotein-dependent transport of newly generated rabies virus in dorsal root ganglion neurons. J Virol 88:14172-83.

60. Potratz M, Zaeck LM, Weigel C, Klein A, Freuling CM, Müller T, Finke S. 2020. Neuroglia infection by rabies virus after anterograde virus spread in peripheral neurons. Acta Neuropathol Commun 8:199.

61. Adler B, Sattler C, Adler H. 2017. Herpesviruses and their host cells: A successful liaison. Trends Microbiol 25:229-241.

62. Li C, Xu D, Ye Q, Hong S, Jiang Y, Liu X, Zhang N, Shi L, Qin CF, Xu Z. 2016. Zika virus disrupts neural progenitor development and leads to microcephaly in mice. Cell Stem Cell 19:120-6.

63. Brasil P, Pereira JP, Jr., Moreira ME, Ribeiro Nogueira RM, Damasceno L, Wakimoto M, Rabello RS, Valderramos SG, Halai UA, Salles TS, Zin AA, Horovitz D, Daltro P, Boechat M, Raja Gabaglia C, Carvalho de Sequeira P, Pilotto JH, Medialdea-Carrera R, Cotrim da Cunha D, Abreu de Carvalho LM, Pone M, Machado Siqueira A, Calvet GA, Rodrigues Baião AE, Neves ES, Nassar de Carvalho PR, Hasue RH, Marschik PB, Einspieler C, Janzen C, Cherry JD, Bispo de Filippis AM, Nielsen-Saines K. 2016. Zika virus infection in pregnant women in Rio de Janeiro. N Engl J Med 375:2321-2334.